

### 3. FUNDAMENTAL THEORY AND METHODOLOGIES

#### 3.1 SCOPE

In this chapter, the fundamental theory underpinning the techniques covered in the present study, as well as methodologies with regard to the determination of input loading, structural fatigue design and testing of vehicular structures, are presented. The chapter firstly deals with the various analysis and testing methods, involved in vehicle structural design and assessment and then discusses the techniques used to determine inputs for these methods.

The various methods and techniques described in this chapter are summarised at the end of the chapter. In particular, the fatigue design methods, as opposed to the testing methods, are contextualised using a diagram. The framework for this diagram is depicted in Figure 3-1. Load inputs are obtained from either measurements, or simulation. These loads are used as inputs for stress analyses, which may be either quasi-static, or dynamic, as well as either in the time domain, or in the frequency domain. The outputs of these analyses are then used in fatigue analyses.

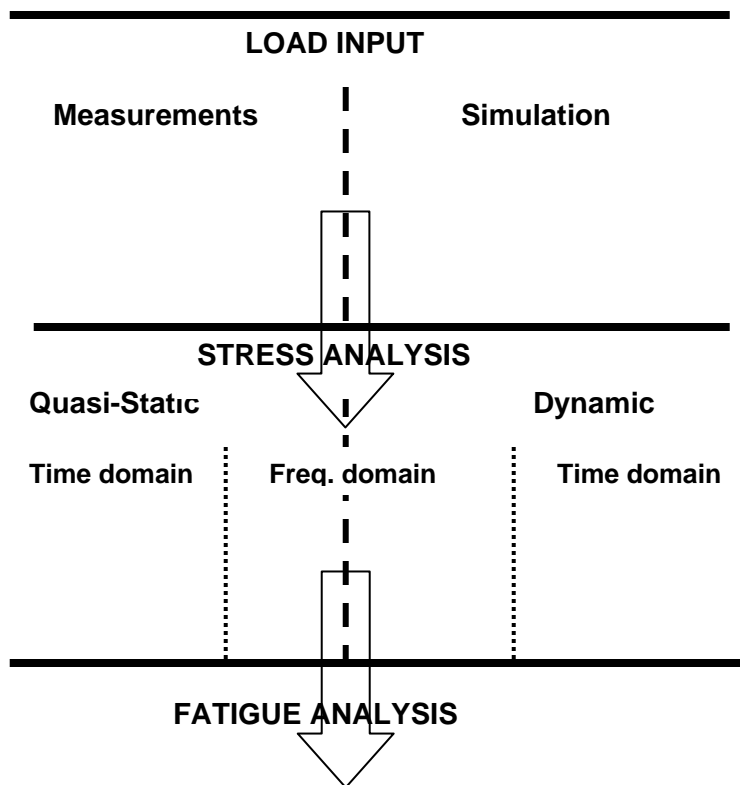


Figure 3-1 Framework for Summary of Fatigue Design Methods

## 3.2 FINITE ELEMENT ANALYSIS

### 3.2.1 General

The finite element method has become an indispensable tool for the design of vehicle and transport structures. Computing power and software sophistication have increased dramatically over the past decades, bringing the technology into the economic grasp of most of the transport industry. It is the present author's experience that there are some transport equipment manufacturers, even in Europe and the USA, which still regard the finite element method as 'high-tech' and therefore still rely on hand-calculations. A possible reason for this is that the method is considered to be inaccurate and therefore not worth the additional effort. One of the principal causes of these inaccuracies, albeit not commonly thus understood, may be the undefined input loading.

It would be defensible to state that using the finite element method instead of hand-calculation methods, or sticking to existing designs, is indeed not worth the additional effort unless input loading is well defined. In cases where high volumes imply high risks, and/or the market is very competitive, demanding lighter and more durable structures, such as in the automotive industry, finite element methods and testing have been extensively used and comprehensive efforts are expended in defining input loading.

In the following sub-sections, some aspects of the Finite Element Method are discussed, with specific reference to its capability of calculating variable stresses/strains, resulting from variable input loads, which then may be used to perform fatigue calculations.

### 3.2.2 Static Load Analysis

#### 3.2.2.1 General

The use of static load finite element analyses in the design process of vehicular structures are commonplace and well documented. In many instances design codes would prescribe static design loads, where fatigue and dynamic considerations are catered for by prescribing large safety factors.

More sophisticated methods are also employed, staying within the economic domain of static analyses, where dynamic stress responses, used for detailed fatigue analysis, are calculated. These methods are called 'quasi-static' and are described in the following subsections.

#### 3.2.2.2 Quasi-static finite element analysis

The basic quasi-static finite element analysis method, described by Bishop and Sherratt (2000) and in the MSC.Fatigue 2003 User's Manual (2002), involves calculating the stress response ( $\sigma_{ij}$ ) for all elements ( $i$ ), or of critical elements ( $i$ ), caused by applying static unit loads ( $L_{j-unit}$ ), one at a time, for all loads acting on the structure.

These results are used to establish a quasi-static transfer matrix  $[K]$  between element stresses and loads. Known time histories of each load ( $L_j(t)$ ) are then multiplied with the inverse of the transfer matrix, achieving, by the principle of superposition, stress time histories ( $\sigma_i(t)$ ) at each element (i):

$$[K] = [\sigma_{ij}]$$

$$\{\sigma_i(t)\} = [K]^{-1} \{L_j(t)\}$$

Eq. 3-1

The method is depicted on the summary framework in Figure 3-2.

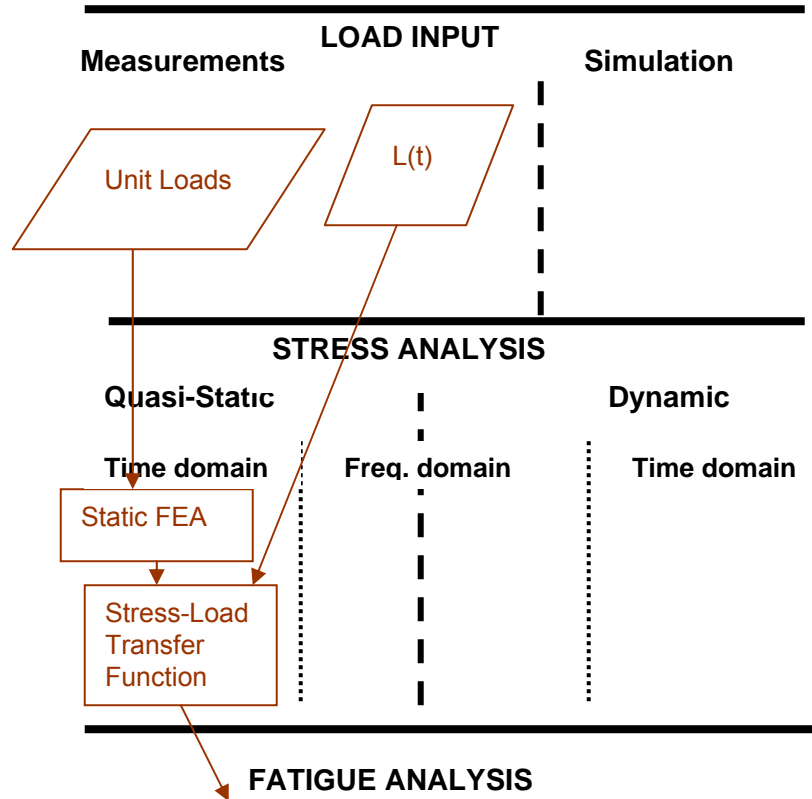


Figure 3-2 Quasi-Static Method

A derivative of this method, employed by Ford Motor Company to perform a durability analysis on a vehicle body-structure in the concept design phase, using the finite element method, is described in Kuo and Kelkar (1995). They state that the absence of detailed design and correct loads at the concept design stage makes upfront fatigue life predictions difficult. A process was developed to overcome these difficulties. The process involves the following:

- Identify relative stress sensitivities by applying unit loads to each body/chassis attachment location, one at a time, using the inertial relief method (the applied load is balanced by an inertial load). A small number of elements are identified which are sensitive to each load (normally in the vicinity of the applied load).

- Identify critical load paths by calculating the fatigue damage at the most critical element for each load, by using the linear relationship between the unit load and the stress at that element to provide a stress history when multiplied with a measured load history. High fatigue damages imply critical load paths. Softening (to reduce loads) or strengthening (to reduce stresses) of the critical load paths can then be applied.
- Identify critical road events by comparing fatigue damages calculated as above for different road events.
- Compute fatigue lives at critical areas by superposition of synchronised time histories for critical load paths and critical road events.

In many instances, inputs for concept design work would however be derived from multi-body simulation (refer to paragraph 3.3), or from measurements performed on previous models.

### **3.2.3 Dynamic Analysis**

#### **3.2.3.1 General**

The most direct way of theoretically assessing the integrity of structures for dynamic and fatigue loading, is by dynamic finite element analysis. The objective would be to solve for the stresses as time functions, when the model is subjected to time series of loads. Additional to the difficulty in defining such loads, there are several restrictions with regard to the use of dynamic finite element analyses, especially for fatigue assessment. These are dealt with in this subsection. It is due to these restrictions that quasi-static methods, some dealt with in this chapter and others presented as part of the present study, are required to be able to perform finite element based fatigue analyses in practice.

#### **3.2.3.2 Explicit and implicit codes**

There are several finite element techniques employed for dynamic analysis of vehicle structures. Explicit codes assume small displacements, which makes it impossible to include the relatively soft suspension in the same model as the relatively stiff structure. The input forces of the suspension onto the structure therefore need to be defined. Implicit codes are able to circumvent this restriction, as the solution is achieved by iteration, but demands on computing power are extreme for large models. Such codes are therefore normally only used for analysis of dynamic events of short duration, such as crash worthiness analyses.

#### **3.2.3.3 Direct integration method**

A further differentiation may be made for explicit codes in terms of the solving method, according to Bathe (1996) and Bishop and Sherratt (2000). One group of methods uses the direct integration method (called 'dynamic transient analysis' by Bishop), solving for the displacements after each small time increment by direct integration. A complete analysis is therefore performed at each time step, except for the compilation of the mass, damping and stiffness matrices, which need only be computed once. Again, the computing power demands are high, normally restricting such analyses to simulation durations of minutes, if not seconds.

The usefulness of such short duration analyses for fatigue assessment purposes is then questionable. Only if the short duration input loading is representative of operational

loading, such as may be the case if the loading is stationary random, could such analysis results be useful. The direct integration method is depicted on the summary framework in Figure 3-3. Load inputs to this method may be obtained through measurements or simulation.

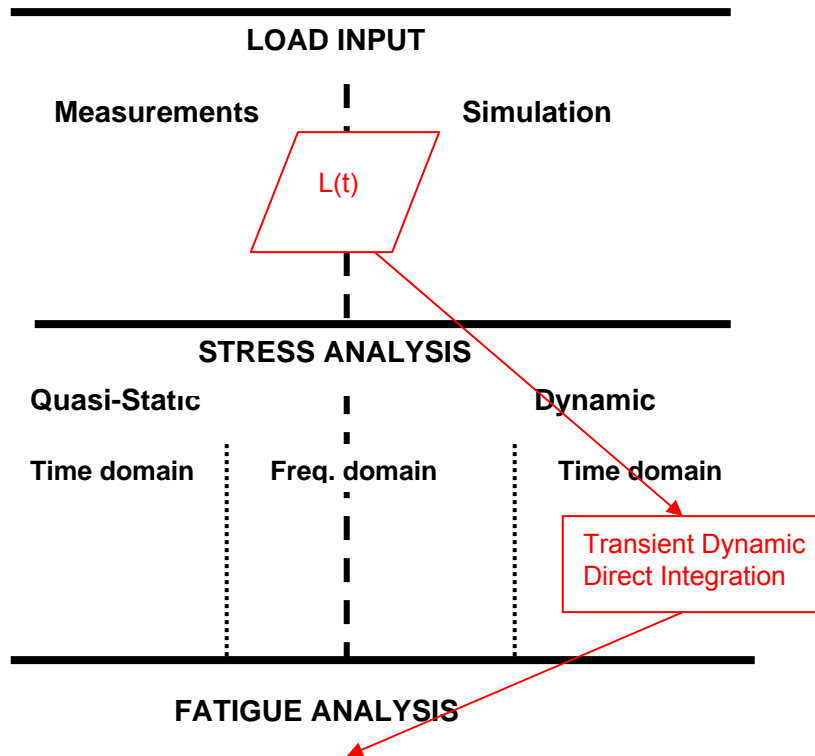


Figure 3-3 Direct Integration Method

#### 3.2.3.4 Modal superposition

A further solving method involves the superposition of forced response mode shapes (the deformed shapes of the structure when vibrating at its natural frequencies), calculated in either the time domain, or the frequency domain, for each eigenvalue solution partially excited by the input loading spectra. The basis of the method is described in various text books, e.g. by Bathe and Wilson (1976). A dynamic system may be described by the following equilibrium equation:

$$[m]\{\ddot{u}\} + [c]\{\dot{u}\} + [k]\{u\} = \{p\}$$

with  $u$  = displacement

$m$  = mass

$c$  = damping

$k$  = stiffness

$p$  = excitation loading

Eq. 3-2

In general, the  $m$ ,  $c$  and  $k$  matrices would have non-zero coupling terms so that solving the equation in the above form would require simultaneous solution of  $N$  equations in  $N$  unknowns ( $N$  being the number of degrees of freedom of the system).

The first step of the modal superposition method is to obtain the natural frequencies ( $\omega_r$ ) and modes ( $\phi_r$ ) of the system, by solving the following equation:

$$([k] - \omega_r^2 [m])\{\phi\}_r = \{0\}$$

**Eq. 3-3**

The modes are then collected to form the modal matrix,  $[\Phi] = [\phi_1 \phi_2 \phi_3 \dots \dots]$ .

The key step is to introduce the coordinate transformation:

$$\{u\} = [\Phi]\{\eta\} = \sum_r \phi_r \eta_r$$

$\eta_r =$  principal coordinates

**Eq. 3-4**

Substituting Eq. 3-4 into Eq. 3-1 and premultiplying with  $[\Phi]^T$  gives the equation of motion in principal coordinates, namely:

$$[M]\{\ddot{\eta}\} + [C]\{\dot{\eta}\} + [K]\{\eta\} = \{P\}$$

with  $\eta =$  principal coordinates

$$[M] = [\Phi]^T [m] [\Phi]$$

$$[C] = [\Phi]^T [c] [\Phi]$$

$$[K] = [\Phi]^T [k] [\Phi]$$

$$\{P\} = [\Phi]^T \{p\}$$

Due to the orthogonality of the principal coordinate system, the mass and stiffness matrices are diagonal. Therefore, in the case of zero damping, or in the special case where the modal damping matrix is also diagonal, the equations of motion are uncoupled. The total response ( $\eta$ ) can then be obtained as a superposition of the response due to initial conditions alone and the response due to the excitation alone.

The economy of the modal superposition method in comparison with the direct integration method is realised if the system response involves only a relatively small subset of the modes of the system.

Two solution methods are discussed, both using mode truncation.

#### 3.2.3.4.1 Mode-Displacement Solution

In this case, the displacement ( $u$ ) is approximated by:

$$\{u\} = [\Phi]\{\hat{\eta}\} = \sum_{r=1}^{\hat{N}} \phi_r \eta_r$$

$\eta_r =$  principal coordinates

$\hat{N} =$  number of truncated modes  $< N$

**Eq. 3-5**

The principal coordinates are then solved from the following uncoupled equations:

$$\begin{aligned}
 [M_r]\{\ddot{\eta}_r\} + [K_r]\{\eta_r\} &= \{P_r\} \\
 \text{with } r &= 1, 2, 3, \dots, \hat{N} \\
 [M_r] &= [\phi_r]^T [m] [\phi_r] \\
 [K_r] &= [\omega_r^2] [M_r] \\
 \{P_r\} &= [\phi_r]^T \{p\}
 \end{aligned}$$

**Eq. 3-6**

It is often found that the mode-displacement solution fails to give accurate results. Convergence may be slow and many modes may be required to give accurate results, thereby negating the economy advantage over the direct integration method. Modes of the elements through which the loads are transferred into the structure also need to be included, otherwise the structure is mathematically 'cushioned' from the loads.

#### 3.2.3.4.2 Mode-Acceleration Solution

A method with superior convergence properties is the mode-acceleration method (MAM), described by Rixen (2001). Eq. 3-1 (without damping) is rearranged as follows:

$$\begin{aligned}
 [m]\{\ddot{u}\} + [k]\{u\} &= \{p\} \\
 \therefore \{u\} &= [k]^{-1}(\{p\} - [m]\{\ddot{u}\})
 \end{aligned}$$

**Eq. 3-7**

Differentiating Eq. 3-5 twice and substituting into Eq. 3-7:

$$\{u\} = [k]^{-1}\{p\} - [k]^{-1} \sum_{r=1}^{\hat{N}} [m] \phi_r \ddot{\eta}_r$$

but,

$$[k]^{-1}[m] = \left[ \frac{1}{\omega_r^2} \right]$$

$$\therefore \{u\} = [k]^{-1}\{p\} - \sum_{r=1}^{\hat{N}} \frac{1}{\omega_r^2} \phi_r \ddot{\eta}_r$$

**Eq. 3-8**

The first term in the above equation is the pseudo-static response, while the second term superimposes the effects of the truncated number of modes. The superior accuracy of this method compared to the mode-displacement method (MDM), can be attributed to the fact that modes disregarded (normally the higher frequency modes, which are required to construct the rigid body displacements), leading to the inaccuracies of the MDM, are implicitly accounted for by the first term of Eq. 3-8, that represents such rigid body displacements.

Ryu et al. (1997) describe the application of the MAM to compute dynamic stresses on a vehicle structure for fatigue life prediction. Input loads are obtained from Multi Body Dynamic Simulation of the vehicle traversing a ground profile. Input loading may also be obtained through measurements. The modal superposition method may be employed in either the time domain, or the frequency domain.

The modal superposition method is depicted on the summary framework in Figure 3-4.

This method was employed in one of the case studies, when it was found that complex modes were excited.

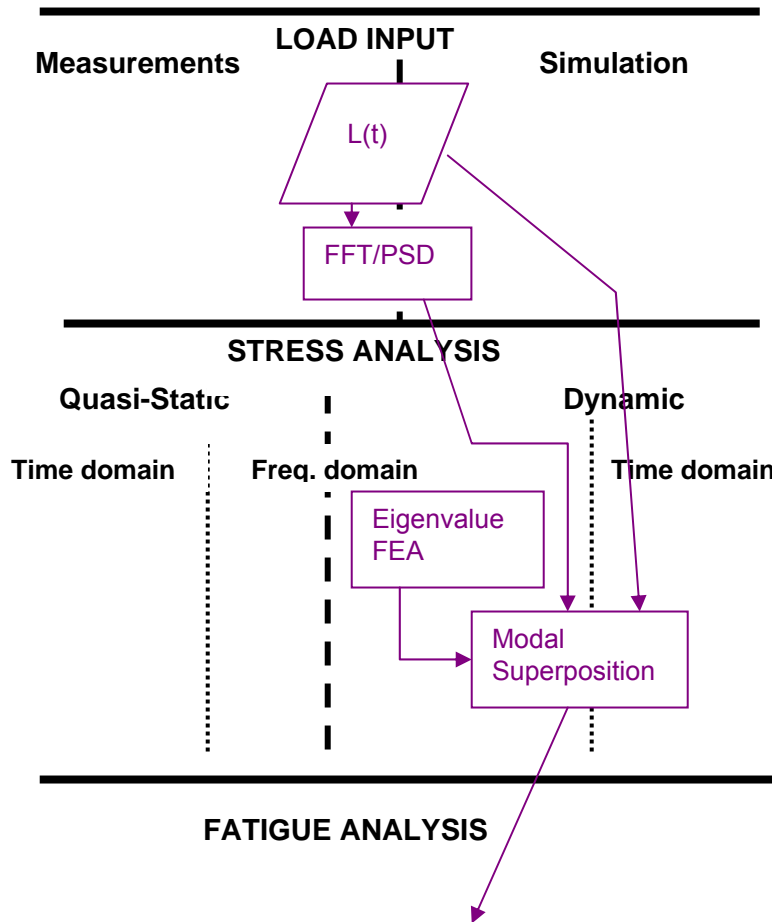


**Figure 3-4 Modal Superposition Method**

### 3.2.3.5 Frequency domain analysis

A third method, called ‘vibration (fatigue) analysis’ by Bishop, involves calculating power spectrum densities of the stresses using input power spectrum densities and cross power spectrum densities, as well as transfer functions computed from the finite element model. This method requires that the input data is stationary random and complicates the fatigue analysis (as described in paragraph 3.4.5), but allows for economic analysis, even for a large number of load sequences. The vibration fatigue method is depicted on the summary framework in Figure 3-5.

### 3.2.3.6 Static condensation

To reduce the calculation effort required, a smaller model can be obtained via static condensation (Aja (2000)) to include only the carefully chosen degrees of freedom required to fully describe the important mode shapes. Back-substitution is then performed after modal superposition to obtain stress and deformation results as functions of time or frequency.



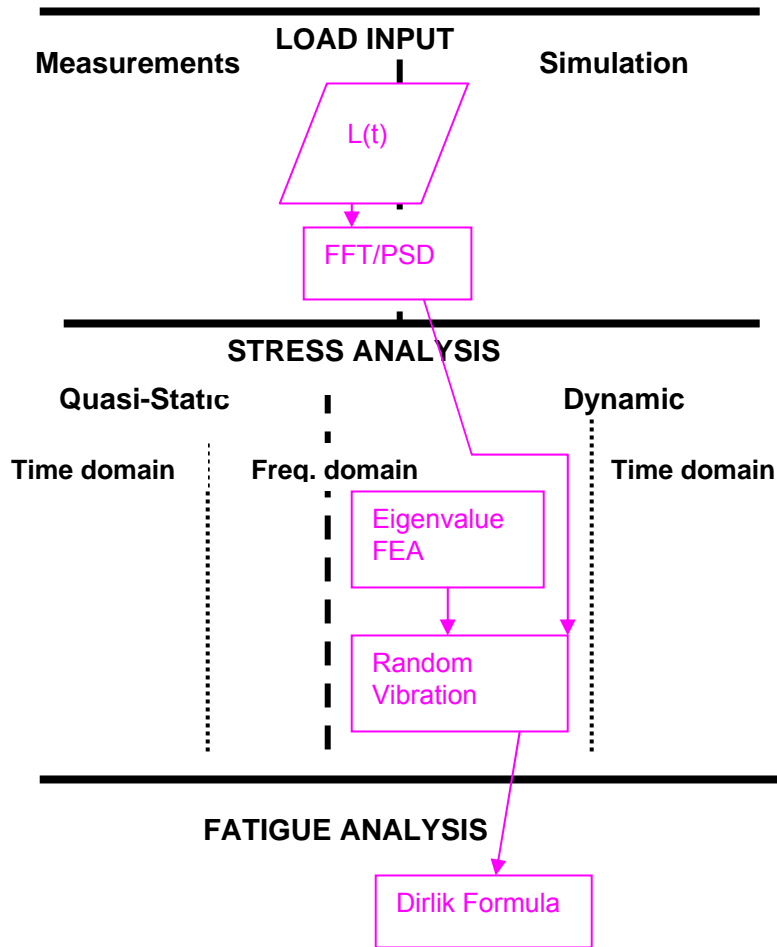


**Figure 3-5 Random Vibration Method**

### 3.2.3.7 Inputs to dynamic analysis

In most cases, inputs for dynamic analyses will be obtained from measurements. On vehicles, the quantities that are typically measured, are accelerations, displacements and/or forces.

#### 3.2.3.7.1 Force inputs

Should forces have been measured, direct solving of the equilibrium equation (Eq. 3-2) can be performed, since the unknown displacements are on one side of the equation. The measured forces, represented by the  $L(t)$  block in the diagrams in Figure 3-2 to Figure 3-5 before, are used as inputs to the various methods.

#### 3.2.3.7.2 Acceleration inputs

It is normally difficult to directly measure forces introduced through the suspension of a vehicle to the vehicle structure. Accelerations are often measured. Direct solving of Eq. 3-2 is then not possible, since prescribed motion terms are part of the  $\{\ddot{u}\}$  vector on the left-hand side of the equation. Three methods may be used to circumvent these problems, according to the MSC/NASTRAN User's Guide.

- Large mass-spring method: This method entails adding an element with a large mass or stiffness at the point of known acceleration. Large forces, calculated as the large mass multiplied by the desired accelerations (or stiffness multiplied by known displacements) are applied to obtain the required motion. The method is not exact and may produce various errors if used with inputs required at more than one point.
- Relative displacement method: This method entails input accelerations defined as the inertial motion of a rigid base to which the structure is connected. The structural displacements are then calculated relative to the base motion. The displacement vector  $\{u\}$ , can be defined as the sum of the base motion  $\{u_o\}$  and the relative displacement  $\{\delta u\}$ :

$$\{u\} = \{\delta u\} + [D]\{u_o\}$$

**Eq. 3-9**

where  $[D]$  is the rigid body transformation matrix that includes the effects of coordinate systems, offsets and multiple directions. If the structure is a free body, the base motions should only cause inertial forces:

$$\begin{aligned} [k][D] &= [0] \\ [c][D] &= [0] \end{aligned}$$

**Eq. 3-10**

Substituting Eq. 3-9 and Eq. 3-10 into Eq. 3-2 yields:

$$[m]\{\delta \ddot{u}\} + [c]\{\delta \dot{u}\} + [k]\{\delta u\} = \{P\} - [m][D]\{\ddot{u}_o\}$$

**Eq. 3-11**

For a vehicle structure, six accelerations may be measured to define the base motion. These may typically be three vertical accelerations (measured on the structures at the two front and one rear suspension mounting points), one longitudinal (it is normally assumed that any rigid position on the vehicle structure would be sufficient to establish the braking and pulling away accelerations), as well as two lateral accelerations, measured on one front and one rear suspension mounting positions.

The vehicle structure would then be fixed to the base at the positions and in the directions of the measured accelerations. The one missing vertical input must then be measured as a force and introduced as a force on one free suspension mounting point. Lateral forces only occur during cornering and it may be assumed that the largest component of such forces would be carried on the inside wheel. Otherwise, two lateral force inputs need to be measured. It is mostly assumed that left and right longitudinal inputs are equal and for pulling away, only the driven wheels are attached to the base, whereas for braking, all four wheel positions may be attached, or only two, with an assumption as to the percentage braking force between front and rear, corrected for by introducing forces at the unattached wheel positions, calculated as the percentage multiplied by the measured longitudinal acceleration, multiplied by the suspended mass of the vehicle. The benefits of this seemingly cumbersome method is a significant saving with regard to the measurement exercise, as well as the avoidance of rigid body modes, which may occur with the other methods due to slight measurement errors.

- Lagrange multiplier technique: This technique requires adding additional degrees of freedom to the matrix solution that are used as force variables for the constraint functions. Coefficients are added to the matrices for the equations that couple the constrained displacement variables to the points at which enforced

motion is applied. The technique produces indefinite system matrices (zero, or relatively small diagonal values) that require special resequencing of variables for numerical stability.

These methods are depicted in Figure 3-6.

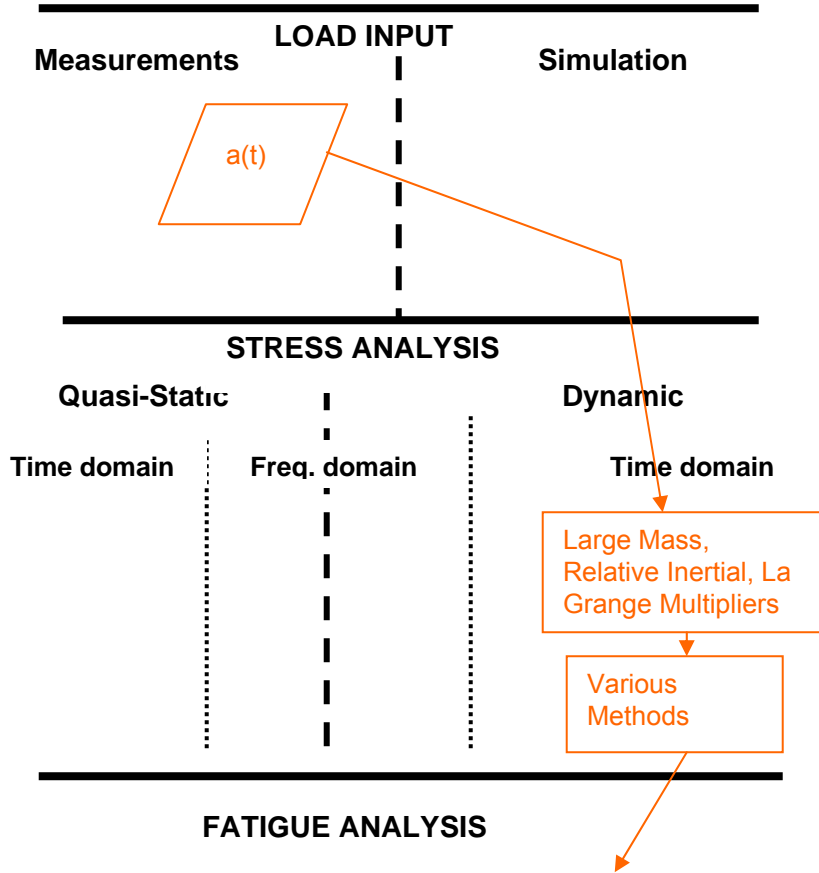


**Figure 3-6 Large Mass, Relative Inertial, La Grange Multipliers Methods**

### 3.2.3.8 Covariance method

A method is described by Dietz et al. (1998), making use of a dynamic simulation model of a train to establish the dynamic loads onto a bogey, after which quasi-static, as well as condensed dynamic finite element analyses, are performed to obtain stress histories for subsequent fatigue analysis.

The distinction is made between linear operational conditions and non-linear events. Linear conditions are assumed when driving straight over a track, where the inputs are small and caused by track irregularities (input into the simulation as spectral densities and output into the dynamic finite element process as a load covariance matrix,  $[P(y)]$ , i.e. in the statistical/frequency domain).

Non-linear events, such as driving through a ramp or over a crossing, are dealt with in the simulation by direct integration in the time domain, producing time histories of input forces to the finite element process.

Due to the large finite element model, it is said to be impracticable to perform dynamic finite element analyses, using the force histories for the non-linear events as inputs. Maximum load time steps are rather identified and quasi-static analyses are performed to calculate the resulting stresses.

For the linear conditions, the covariance matrices of the input forces are used in a condensed dynamic finite element analysis process in the statistical/frequency domain.

A stress load matrix [B] is calculated for only the critical areas of concern, with,

$$[\sigma_c(t)] = [B] [L(t)]$$

**Eq. 3-12**

where  $[\sigma_c(t)]$  are the stress tensors at the critical locations,  $[L(t)]$  are the various input loads (forces and accelerations as a function of time) and [B] contains the stress tensor results from static unit load analyses for each input load, as well as the eigenmode stresses obtained from dynamic finite element analysis. Eq. 3-12 is equivalent to Eq. 3-1 with  $[B] = [K]^{-1}$ .

The time independent stress load matrix allows transformation of the load covariance matrix into a stress covariance matrix:

$$[P(\sigma)] = [B] [P(y)] [B]^T$$

**Eq. 3-13**

Although the resulting stress covariance matrix only contains information about the amplitude distribution of stresses, the number of cycles can be derived by assuming a probability density function for a stationary random process, thereby allowing fatigue analyses to be performed at the critical positions.

This method is therefore a quasi-static method in the frequency domain.

This method is depicted in Figure 3-7.

### 3.2.4 Sources of inaccuracies

Bathe (1996) and Rhaman (1997) discuss sources of inaccuracies when performing finite element analyses. Apart from inaccuracies occurring due to inaccurate input loads, the following are important:

- Discrepancies between model and real structure
- Boundary conditions
- Simplifying assumptions
- Element type
- Mesh refinement
- Material properties

Any of these, or a combination, could render finite element analysis results unusable.

### 3.2.5 Summary

As is clear from the above discussion, dynamic finite element analysis of vehicle structures, is a non-trivial problem. Several choices exist as to which method to apply,

mostly dependent on the type of input data available. Generally, it is not practical to perform dynamic analyses to obtain fatigue stresses, unless stationary random data is assumed, and/or the model is condensed. Measurements performed to obtain input data for these analyses, require careful planning. Due to economy considerations, as well as the fact that dynamic analysis requirements would mostly be too complex for inclusion in design codes and standards, quasi-static methods are mostly employed, therefore the emphasis of the present study.

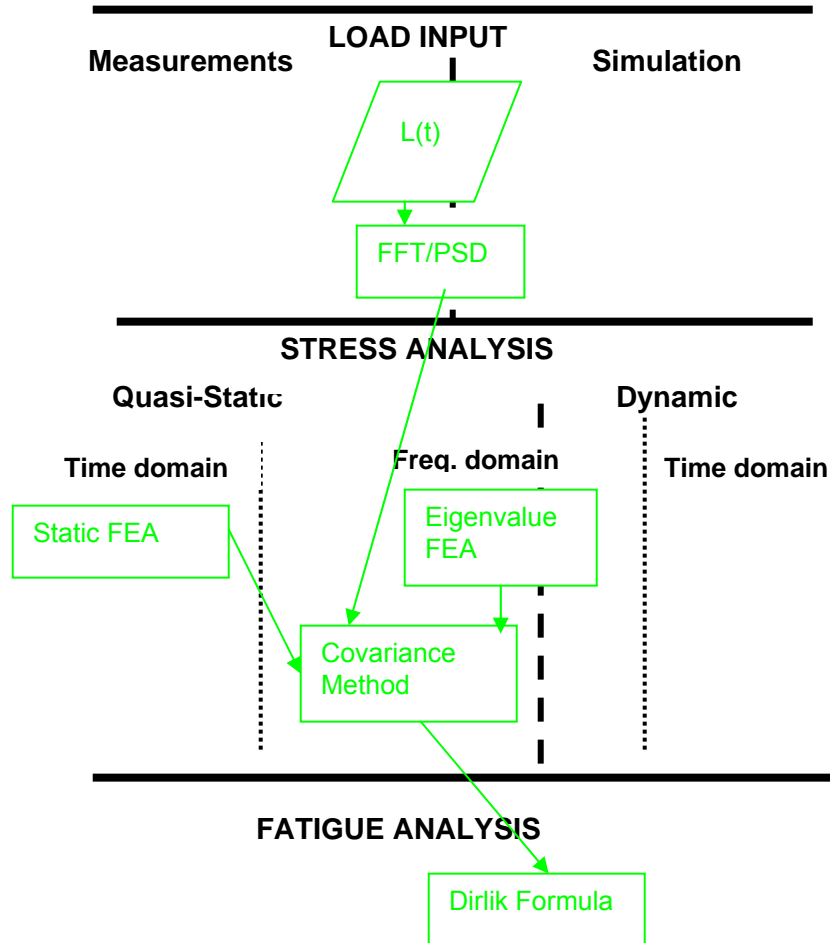


Figure 3-7 Covariance Method

### 3.3 MULTI-BODY DYNAMIC SIMULATION

An important technique to establish dynamic input loading for vehicle structures when measurements are not possible, is multi-body dynamic simulation. A dynamic (mass-spring-damper) model of the vehicle system is constructed. The traversing of the vehicle over terrain with known statistical or geometric profiles (such as digitised proving ground section profiles) is then simulated to solve for the dynamic input loading. These loads may then be applied to finite element models.

Examples of this process are reported on by Dietz et al. (1998) (dealt with in the previous subsection) and by Oyan (1998), where the fatigue life prediction for a railway bogie and a passenger train structure is performed using dynamic simulation.

For trackless vehicles, one of the fundamental difficulties for accurate dynamic simulation of input loads, is related to the complexity of modelling of the tyres. Analytical tyre models are described by Captain et al (1979) and tyre modelling by finite element methods is discussed by Faria et al. (1992). Mousseau states in SAE Fatigue Design Handbook (1997), that simplified tyre models may lead to significant errors in terms of simulating durability loading.

For the durability assessment of a complete body structure of a vehicle using finite element methods, dynamic simulation is often employed to solve for the high number of loads acting on body attachment locations, due to the practical difficulties in measuring these loads, as discussed by Gopalakrishnan and Agrawal (1993). Measured wheel loads, using a specialized loadcell, are introduced to a dynamic model, which then solves for the attachment point loads.

The same process may be followed, using measured wheel accelerations, as described by Conle and Chu (1991). Difficulties are however usually encountered with the double integration of the acceleration signals to obtain displacements. Table 3-1 summarises the different types of dynamic simulation applications.

**Table 3-1 Types of Dynamic Simulation Applications**

	MULTI-BODY DYNAMIC SIMULATION		
	Type 1	Type 2	Type 3
<b>Purpose</b>	To obtain FEA load inputs without the availability of measurements	To obtain FEA load inputs on suspension hard points	To obtain FEA load inputs on suspension hard points
<b>Input</b>	Digitised road profiles	Measured spindle loads	Measured wheel accelerations
<b>Difficulty</b>	Require complex tire model	Require specialised loadcell	Double integration of measured accelerations present problems

The multi-body dynamic simulation process is depicted in Figure 3-8.

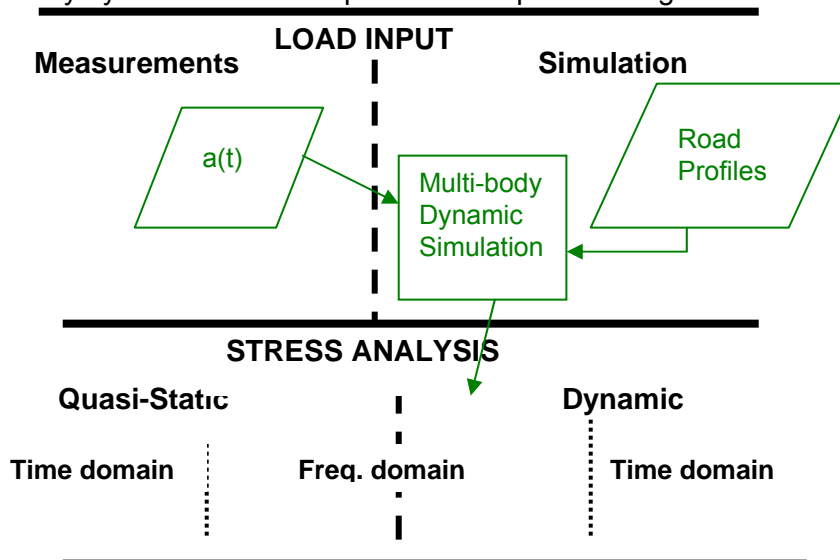


**Figure 3-8 Multi-body Dynamic Simulation Method**

### 3.4 DURABILITY ASSESSMENT

#### 3.4.1 General

According to Dressler and Kottgen (1999), six different fatigue durability assessment methods, adapted to different development stages, are currently used in the vehicle industry:

- Test drives on public roads.
- Drives on test tracks.
- Laboratory testing with edited time histories.
- Laboratory testing with synthetic service loading.
- Numerical analysis based on the nominal stress approach (stress-life).
- Numerical analysis based on the strain-life approach.

#### 3.4.2 Fatigue Analysis

##### 3.4.2.1 Stress-life approach

The stress-life approach is described by Bannantine et al. (1990). The approach is based on the experimentally established material fatigue response curve (the SN curve, or Wöhler curve – see Figure 3-9), which plots number of cycles (N) or reversals (2N) to failure (mostly defined as the initiation of an observable crack) vs nominal stress range ( $\Delta\sigma$ ) or amplitude ( $\sigma_a$ ).

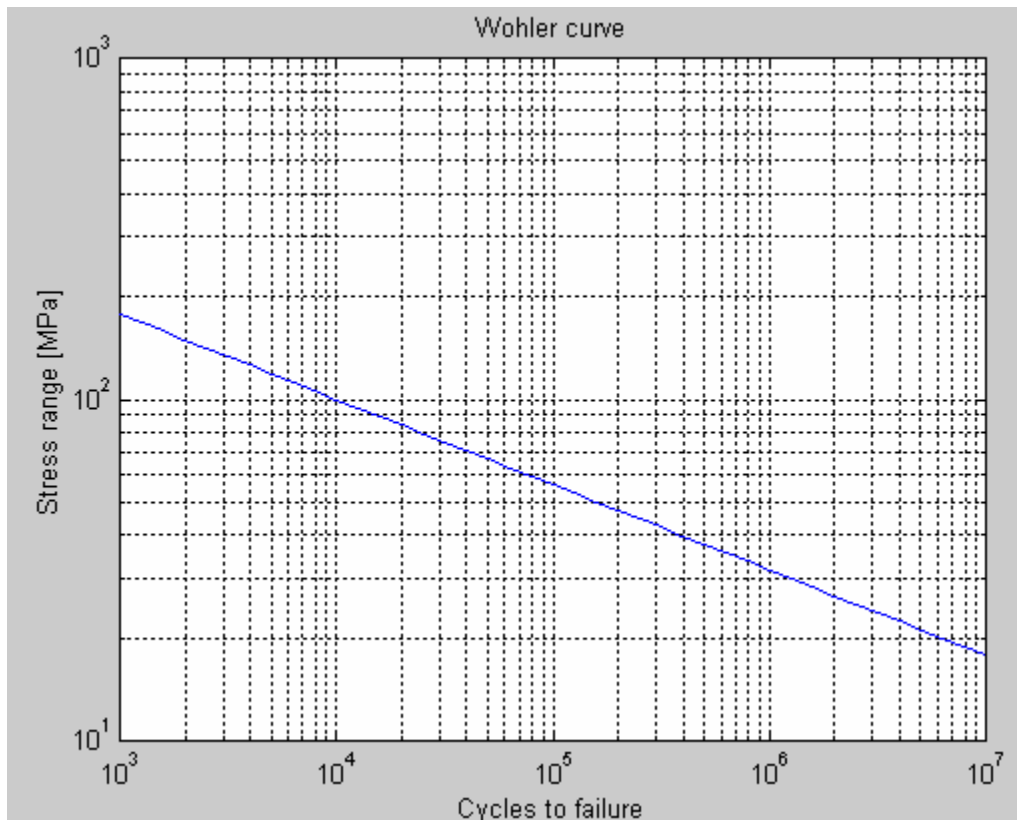


Figure 3-9 Typical SN (or Wöhler) curve

On a log-log plot, an approximate straight line is observed, resulting in a power-law relationship:

$$\Delta\sigma = S_f N^b$$

$S_f$  = fatigue coefficient  
 $b$  = fatigue exponent

**Eq. 3-14**

### 3.4.2.2 Strain-life approach

The strain-life or local strain approach is essentially an extension of the stress-life approach into the elastic-plastic regime. The theory is described by Bannantine et al. (1990). The strain life equation describes the local strain range ( $\Delta\varepsilon$ ) as a function of four material parameters, as well as the number of cycles to failure ( $N$ ):

$$\frac{\Delta\varepsilon}{2} = \frac{S_f}{E} (2N)^b + \varepsilon_f (2N)^c$$

with :  $S_f$  = Fatigue strength coefficient  
 $\varepsilon_f$  = Fatigue ductility coefficient  
 $b$  = Fatigue strength exponent  
 $c$  = Fatigue ductility exponent

**Eq. 3-15**

The local strain range is expressed as a function of the local stress range ( $\Delta\sigma_l$ ) using the cyclic stress-strain relationship:

$$\frac{\Delta\varepsilon}{2} = \frac{\Delta\sigma_l}{2E} + \left( \frac{\Delta\sigma_l}{2K'} \right)^{1/n'}$$

with :  $n'$  = Cyclic strain hardening exponent  
 $K'$  = Cyclic strength coefficient  
 $E$  = Elasticity modulus

**Eq. 3-16**

The stress and strain ranges at a local stress concentration are related to nominal stress range ( $\Delta\sigma$ ) and strain range ( $\Delta\varepsilon$ ) through the Neuber equation (see Neuber (1969)):

$$\sqrt{\Delta\sigma_l \Delta\varepsilon} = K_t \sqrt{\Delta\sigma \Delta\varepsilon E}$$

**Eq. 3-17**

with the stress concentration factor =  $K_t$ .

The process to calculate fatigue damage is a more complex one, with the point by point calculation of the local stress-strain history by simultaneous numerical solution of the above equations, as described in the SAE Fatigue Design Handbook (1997).

The strain-life approach is considered to be a better model of the fundamental mechanism of fatigue initiation compared to the stress-life approach, since it takes



account of the notch root plasticity, with the cyclic plastic strain being the driving force behind the fatigue mechanism.

For high-cycle fatigue applications, the stress-life and strain-life techniques converge, since the effects of plasticity would be small (i.e. the first term of Equation 3-15 would be dominant and the second negligible). The transition between high-cycle fatigue and low-cycle fatigue is defined by the intersection point of the curves representing these two components, named the transition life. This transition life is found to be material dependent, increasing with decreasing hardness. According to Bannantine et al. (1990), a medium carbon steel in a normalized condition would have a transition life of 90 000 cycles (implying that the plastic term would still significantly contribute for a number of cycles of more than  $10^5$ ), whereas the same steel in a quenched condition would have a transition life of 15 cycles (implying that the plastic term would not be significant).

It may be argued that, in the case of vehicle structures, where the number of cycles to failure would typically be millions (for example, the rigid body natural frequency of the body on its suspension may be typically 2 Hz, implying that a million cycles would occur in 140 hours), stress life methods should often suffice. The loading are however of a stochastic nature and therefore, the number of cycles are not so simply defined. The major contributors to damage accumulated on a specific component, may be large, impact driven stress response, induced during events that occur infrequently.

### **3.4.2.3 Fracture mechanics approach**

The fatigue mechanism is normally described as consisting of two phases, namely the crack initiation phase, as well as the crack propagation phase. This is however an engineering distinction, rather than a physical distinction, due to the difficulty of measuring very small cracks. The stress- and strain-life approaches dealt with above, are usually employed to predict the number of cycles to either separation failure (initiation plus propagation), or initiation of a visible (measurable) crack, depending on the definition of the life to failure.

The propagation of a crack is governed by the Paris equation (Broek (1985)):

$$\frac{da}{dN} = C \Delta K^m$$

with : C, m = material properties

$$\frac{da}{dN} = \text{crack growth per cycle}$$

$\Delta K$  = stress intensity range

**Eq. 3-18**

The fracture mechanics approach finds very few applications in vehicle structural analysis, even though for welded components the life to failure is dominated by the propagation phase, due to pre-existing defects. The fatigue analysis of welded components, however is performed using an approach similar to the stress-life approach, as explained in the next section.

### **3.4.2.4 Fatigue of welded components**

The fatigue analysis of welded components, very important in vehicular structures, is based on original work done by Gurney (1976). SN-curves, equivalent to the material

properties used in the stress-life method, are derived from extensive tests performed on different weld joint specimens.

#### 3.4.2.4.1 Reference stress

For most joint classifications, the reference stress used in the SN-curve is the nominal principal stress in the direction indicated by the joint classification detail, at the weld toe and uninfluenced by the weld geometry itself. It is therefore a stress that does not exist in reality. The weld geometry formed part of the component test and its effect is therefore accounted for in the SN-curve. Stress concentrations other than due to the weld geometry need to be additionally accounted for. The proper use of strain gauge measured stresses or finite element results require careful consideration. A strain gauge placed at the weld toe would include weld geometry effects and would therefore yield conservative results. Stresses measured too remotely may exclude bending stress or stress concentration gradients and therefore need to be extrapolated to the weld toe. The same principle applies to stresses calculated with finite element methods. Shell element models do not include the geometry of the weld itself, but for T-joints, will exhibit high stress concentration at the perfectly square and sharp joint, also depending heavily on how fine the mesh is.

Niemi and Marquis (2003) recommend a pragmatic rule, ensuring elements the size of the weld throat next to the joint, where the nominal stress can be taken as the stress in the second element away from the joint.

#### 3.4.2.4.2 Conservativeness

The Gurney paper provides the mean, first standard deviation, as well as second standard deviation curves (the latter curves are mostly used in design codes and implies a probability of failure of 2.3 %). When performing failure predictions to be compared to actual failures, it would be more accurate to use the average curves. The stress range values for a class F2 weld (fillet weld of T-joint across stressed member) at 2 million cycles are as follows:

- Mean = 85 MPa
- First standard deviation = 71 MPa
- Second std = 60 MPa

There is therefore typically a two classifications jump from the 2.3% curve to the average curve.

#### 3.4.2.4.3 SN-curve gradient (fatigue exponent)

In most fatigue design codes (e.g. ECCS (1985), BS 8118 (1991)), the fatigue exponent for all welded joints is generalised to be  $b = -0.333$ . It is argued that this generalisation is possible due to the fact that  $b = -1/m$ , with  $m$  being the exponent of the Paris equation (approximately 3 for many metals), because the fatigue life of a welded joint is governed by propagation of a pre-existing defect.

Integration of Eq. 3-18 yields:

$$N = C \Delta \sigma^{-m} \int_{a_i}^{a_f} (\sqrt{\pi a})^{-m} da$$

$$\Delta \sigma \propto N^{-\frac{1}{m}}$$

**Eq. 3-19**

A value of  $b = -0.333$  is therefore often used when performing relative damage calculations for vehicle structures when weld failures are expected.

#### 3.4.2.4.4 Mean stress

No mean stress effects need to be taken into account, since it is argued that the as-welded specimens would have had residual welding stresses close to yield stress already.

#### 3.4.2.4.5 Design standards

Numerous fatigue design standards or codes are based on the above method. For steel, the European code, ECCS (1985) and for aluminium the British code BS 8118 (1991), are employed in the present study.

#### 3.4.2.4.6 Equivalent constant range stress

The steel code uses the concept of an equivalent constant range stress at an arbitrary number of applied cycles to replace random stress signals after rainflow counting, before estimating fatigue life. This is done on the basis that the equivalent stress range and number of cycles combination should induce the same damage as the random signal. The formula is derived in Section 5.4.2 in a slightly different format and forms the basis of the Fatigue Equivalent Static Load method developed during the present study.

In both codes, the classification of welds are denoted according to their stress range strengths in MPa at 2 million cycles, instead of the symbols A,B,C,.. employed by Gurney. This is the main reason for calculating equivalent constant range values at 2 million cycles.

#### 3.4.2.4.7 Hot-spot stress

Leever (1983) and Stephens et al. (1987) describe methods using the 'hot-spot' stress for fatigue calculations. This is of importance when a complex joint which cannot be classified according to the design codes, requires analysis. The hot-spot stress is the maximum principal stress at the weld toe, which may be calculated by finite element analysis with solid elements, which include the weld geometry.

### **3.4.2.5 Fatigue of spot welds**

The fatigue prediction of spot-welds is of importance for vehicle design. Again the essential fatigue mechanism is a crack propagation mechanism, where the initial crack front is in fact the sharp edge formed by the joined plates at the weld boundary. A method similar to the SN approach has been empirically developed (Rupp (1989), Rui et al. (1993)), which makes it possible to use the calculation techniques developed during the present study also for spot-welded structures.

### **3.4.2.6 Multi-axial fatigue**

Chu (1998) states that the need to use multi-axial fatigue methods for non-proportional loading has been recognised by the significant improvement in fatigue life prediction accuracy these analyses yield over the traditional uni-axial method. A methodology is presented, based on the strain-life approach, which includes a three-dimensional cyclic stress-strain model, the critical plane approach, which requires the fatigue analysis to be performed on various potential failure planes before determining the lowest fatigue life, a bi-axial (normal and shear stress) damage criterion, as well as a multi-axial Neuber

equivalencing technique, used to estimate from elastic finite element stress results, the multi-axial stress and strain history of plastically deformed notch areas.

The present study is limited to the use of uni-axial fatigue methods. More accurate determination of input loading (the aim of the present study), may, in many instances, outweigh the inaccuracies caused by neglecting multi-axial effects.

**3.4.2.7 Summary of fatigue analysis methods**

The various Fatigue Analysis methods described in Paragraph 3.4.2 are depicted on the summary diagram in Figure 3-10. All these methods require an intermediate step, collectively named Cycle Counting, to convert frequency domain, or time domain stress histories to stress ranges and numbers of cycles. Methods of Cycle Counting are discussed in the next paragraph. All the Fatigue Analysis methods also require material property inputs, as depicted in the diagram.

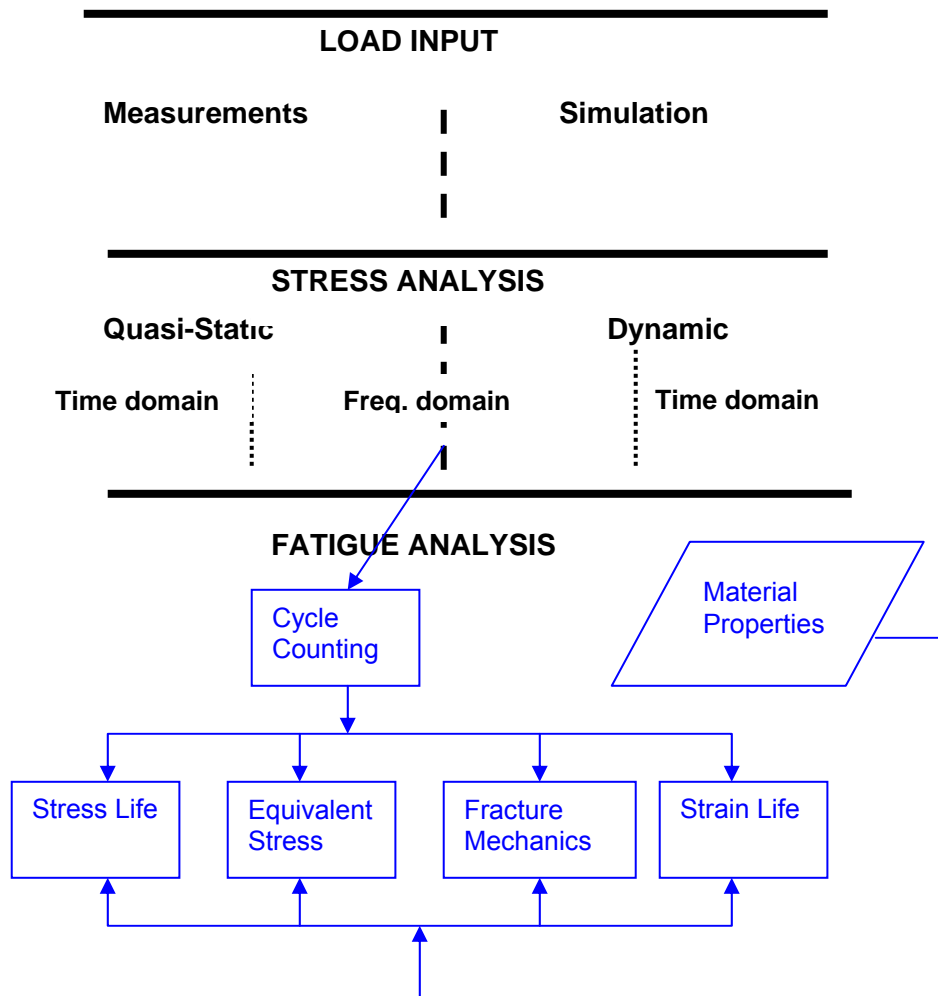


**Figure 3-10 Fatigue Analysis Methods**

### 3.4.3 Cycle Counting

#### 3.4.3.1 Rainflow counting

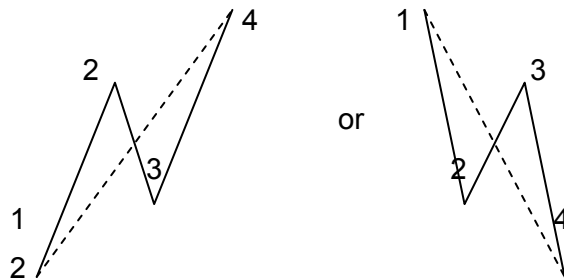
##### 3.4.3.1.1 Hand counting method

The rainflow counting method is described in SAE Fatigue Design Handbook (1997). The original logic of the method was based on the extraction of closed hysteresis loops from the elastic-plastic stress-strain history. The method however logically counts half cycles with different ranges from random stress histories, making it possible to use the stress-life approach and Miner's damage accumulation rule for fatigue life estimation (Miner (1945)).

##### 3.4.3.1.2 Computerised counting method

An algorithm which is more easily computerized, also called the range-pair-range method is described in SAE Fatigue Design Handbook (1997).

In principle, the algorithm searches for a sequential four point pattern shown below, commencing at the first 4 points of the reduced signal (where only peaks and valleys are kept):



Point 1 must be lower or equal to point 3 and point 4 must be higher or equal to point 2 (and the opposite for the mirror pattern).

When a pattern is found, a half cycle is recorded with a range between the values of points 2 and 3. Points 2 and 3 are then deleted and points 1 and 4 connected, as shown by the dashed lines. The algorithm then steps back by 2 points and continues the search. This process continues until the end of the signal is reached. A list of counted cycle ranges ( $\Delta\sigma_i$ ) results, with  $i$  from 1 to the number of half cycles counted.

##### 3.4.3.1.3 Standard counting method

A standardized counting method is prescribed in ASTM E 1049-85 (1989). The method is based on the range-pair-range method, but yields the same results as the rainflow counting method and is usually referred to also as rainflow counting.

##### 3.4.3.1.4 Statistical properties of rainflow counts

The computation of statistical properties of rainflow counts is described by Olagnon (1994).

### 3.4.3.2 Rainflow reconstruction

Measured data is often only available in the compressed fatigue domain (Rainflow matrix) format. For laboratory testing to be performed it is necessary to reconstruct time domain data from the rainflow data, according to Lund and Donaldson (1992). Specialised techniques are required.

### 3.4.3.3 Multi-axial, non-proportional loading

Cycle counting methods for multi-axial, non-proportional loading, are summarized by Dressler and Kottgen (1999). The intention is to count cycles such that a multi-axial fatigue calculation (e.g. according to the critical plane approach) may be performed from reconstructed data. A notch simulation approach is used where a pseudo stress time history is used to compute the full elastic-plastic stress and strain tensor histories required to calculate the fatigue damage in different directions. This pseudo stress ( ${}^e\sigma$ ) at a location ( $s$ ) and time ( $t$ ) is a superposition of the response from ( $n$ ) different load components ( $L_m$ ) acting at time ( $t$ ) on the structure:

$${}^e\sigma_{ij}(t,s) = \sum_{m=1}^n c_{ij,m}(s)L_m(t) \quad \text{Eq. 3-20}$$

where  $c_{ij,m}(s)$  are dimensional proportionality constants similar to stress concentration factors. A number of discrete combinations of these constants are chosen to cover the total range of possible contributions of the different loads to a stress state at any position, which then results in a finite number of rainflow matrices being counted. The stress state at any specific position will then correspond to one of these matrices. Load reconstruction may then be performed, where-after the damage in the most critical direction may be computed using the strain-life approach.

This method also makes it possible to filter non-proportional loading, where only time intervals producing loops smaller than the filter value for all the load projections, are filtered.

### 3.4.4 Damage Accumulation

The process to calculate fatigue damage caused by random loading is based on the linear damage accumulation approach, proposed by Miner (1945). The total damage ( $D$ ) caused by a combination of cycles of different ranges is calculated as the linear sum of the fraction of the applied number of cycles at that range ( $n_i$ ) divided by the number of cycles to failure at that range ( $N_i$ ). Failure is expected if the total damage reaches unity.

$$D = \sum \frac{n_i}{N_i} \quad \text{Eq. 3-21}$$

The process to calculate fatigue damage from random stress histories, is depicted in Figure 3-11 (shown here for the stress-life approach).

### 3.4.5 Frequency Domain Fatigue Life

Methods for estimating fatigue life from frequency domain data are described by Sherratt (1996). Although the fatigue failure mechanism is essentially dependent on amplitudes and number of occurrences (parameters determined through cycle counting from time domain data), data storage space and communication restrictions often imply the need to find more compact data formats, such as the direct storage of real time cycle counted

results, or the statistical information represented by the frequency domain. In the present study, a case study is presented where both these domains were employed.

Data stored in a Power Spectral Density (PSD) format, represents averaged statistical information concerning the energy contained in the original time domain signal at each frequency. Since the energy will be related to amplitudes and the frequencies to number of cycles, intuitively it should be possible to calculate fatigue damage.

A key step is to predict the distribution of peaks and valleys in the time history. For a time history  $x$ , a peak and valley will occur when  $dx/dt = 0$ . A peak will occur when  $d^2x/dt^2$  is negative and a valley if it is positive. There are links between  $x$ ,  $dx/dt$ ,  $d^2x/dt^2$  and various moments of the PSD around the frequency axis. The  $n^{\text{th}}$  spectral moment is defined as:

$$m_n = \int_0^{\infty} f^n G(f) df$$

**Eq. 3-22**

where  $G(f)$  is the value of the PSD as a function of frequency ( $f$ ).

According to statistical theory, the variance of  $x = m_0$  (the area of the PSD, or energy), the variance of  $dx/dt = m_1$  and the variance of  $d^2x/dt^2 = m_2$ . It is normally assumed that  $x$  follows a Gaussian distribution.

It is then possible to derive values for number of cycles vs range as follows:

- Estimate the number of times a given boundary at a value  $\alpha$  will be crossed in one second with  $x$  increasing.
- Apply this at  $\alpha = 0$  to estimate the number of positive-going zero crossings in one second.
- Estimate the number of positive-going zero crossings of  $dx/dt$  in one second. This will be the number of valleys per second and be equal to the number of peaks.
- Use the level-crossing information from the first step to estimate the number of peaks at each level.

The ratio of positive-going zero crossings per second  $N_0$  (step 2 above), to the number of peaks per second  $N_p$  (irregularity factor  $\gamma = N_0/N_p$ ), is a measure of how irregular the time history is. If it is near unity, the record passes through zero after almost every peak and cycles may be formed by pairing every peak with every valley at the same level below (the peak values are therefore an indication of amplitude). This will be the case if the PSD is narrow-band.

In the wide-band case, the assumption which links peaks and valleys at similar levels above and below zero, gives a conservative estimate of damage. This may be understood if it is compared with the rainflow algorithm, which links peaks with valleys closer to it's own level.

An alternative way to calculate damage from PSD data would be to produce time data from it which can be cycle counted directly, using the inverse FFT method (IFFT). For this, phase information needs to be created (not kept by the PSD calculation), by creating a random phase record. The effect of this method is to reduce the conservative damage result for wide-band data by some 20%.

Sherratt (1996) describes the Dirlik formula (refer to Eq. 3-24) which estimates the probability density function (PDF) of rainflow ranges as a function of moments of the PSD. This formula is empirically derived from the results of IFFTs of a number of PSDs with random phases. This formula allows closed form estimation of fatigue damage from PSD data.

It is lastly important to note that a fundamental assumption made when using frequency domain data is that the time data is stationary, meaning that PSDs taken on any partial duration of the data would be similar. This would be true for data obtained from a vehicle travelling on a road of constant roughness, but will certainly exclude transient events, such as hitting a curb.

$$P_{RR}(S) = \frac{(D_1 e^{-Z/Q}) / Q + (D_2 Z e^{-(Z/R)^2/2}) R^2 + D_3 Z e^{-Z^2/2}}{2(m_0)^{1/2}}$$

with :

$P_{RR}(S)$  = PDF of rainflow ranges of S

$$\gamma = \frac{m_2}{(m_0 m_4)^{1/2}}$$

$$x_m = \frac{m_1 m_2^{1/2}}{m_0 m_4^{1/2}}$$

$$D_1 = \frac{2(x_m - \gamma^2)}{x_m + \gamma^2}$$

$$D_2 = \frac{1 - \gamma - D_1 + D_1^2}{1 - R}$$

$$D_3 = 1 - D_1 - D_2$$

$$Q = 1.25 \frac{\gamma - D_3 - D_2 R}{D_1}$$

$$R = \frac{\gamma - x_m - D_1^2}{1 - \gamma - D_1 - D_1^2}$$

$$S = 2m_0^{1/2} Z$$

Eq. 3-23

#### 3.4.5.1 Errors induced by signal processing and cycle counting

Errors induced by signal processing and cycle counting are discussed in the SAE Fatigue Design Handbook (1997) and by Broek (1985). The planning the measurement configuration requires careful consideration of the following aspects:

- Transducer sensitivity, accuracy and range  
It is good practice to perform trial measurements to confirm that, e.g. no overloading would occur, before commencing with actual measurements.
- Sample frequency, aliasing and filtering  
From a frequency domain point of view, the sample frequency should be at least twice the highest frequency of concern contained in the signal. From a time domain point of view, peak definition would be inadequate should the sample



rate be chosen on this basis and sample rates at 5 – 10 times the relevant input frequencies are required. Small errors in defining peak values are amplified when performing fatigue life prediction, due to the fatigue exponent effect.

- Noise protection
- Capacity, resolution and gains
- Strain gauge temperature compensation

Load sequencing is known to have a significant effect on fatigue crack propagation, due to an effect known as crack retardation. Fracture mechanics models exist to take account of this effect, but it is mostly ignored when performing stress-life or strain-life predictions.

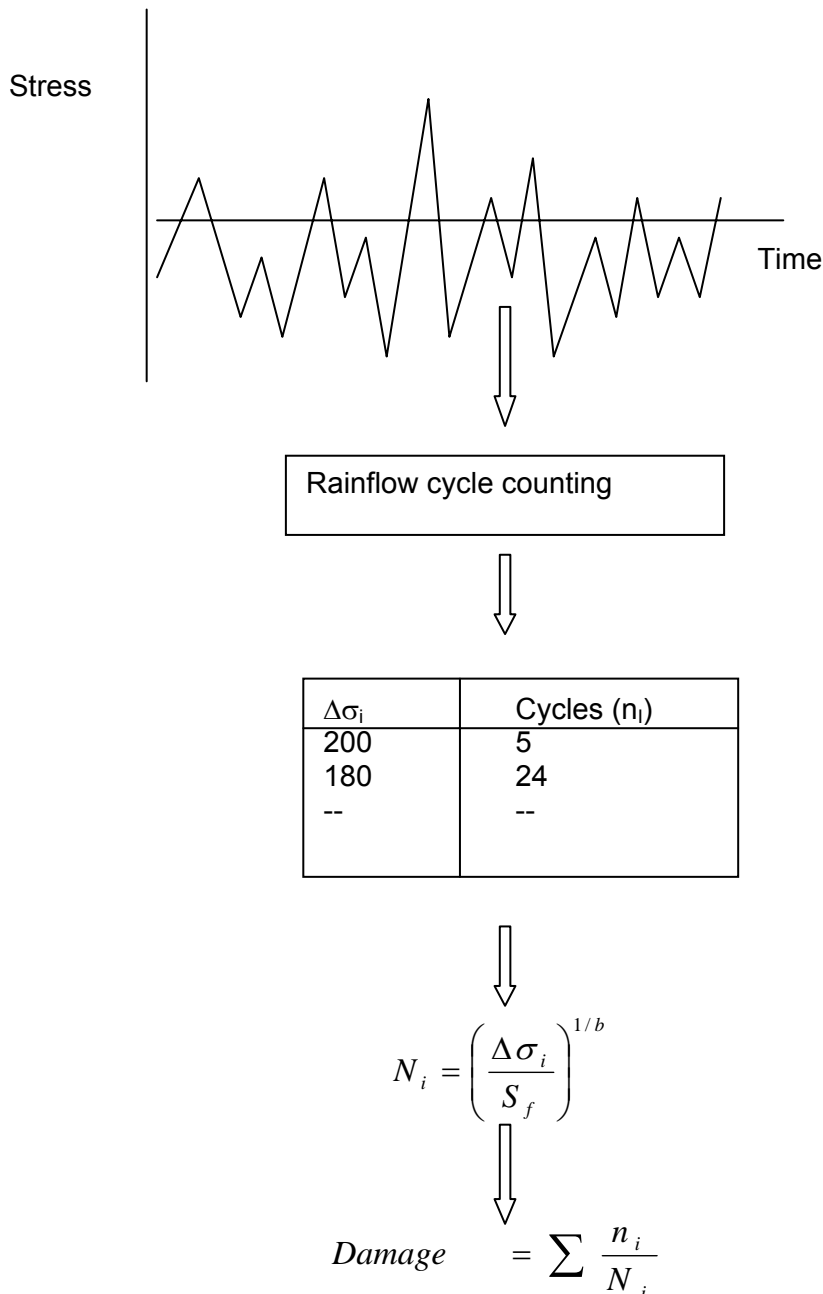


**Figure 3-11 Fatigue damage calculation process**

### 3.4.5.2 Summary of cycle counting methods

The two Cycle Counting methods are depicted on the summary diagram in Figure 3-12. Rainflow counting is performed using time domain data and the Dirlik method is used with frequency domain data.

### 3.4.6 Durability Testing

#### 3.4.6.1 Test development and correlation

##### 3.4.6.1.1 General

Generally, durability qualification testing of engineering systems should conform to two basic requirements for validity, namely, the accurate simulation of possible service failures and failure modes, as well as a known relation between test duration and actual service life. Testing with the purpose to infer reliability data has the additional requirement of having to be able to relate the test results to expected service lifetimes within statistical confidence intervals.

The first requirement implies that simulation of the mission profile in terms of loading conditions, environmental conditions etc. should be sufficiently comprehensive so as to include all possible causes of failure. It also implies that, should the test be accelerated, the failure modes that may occur in service would still be induced during the test.

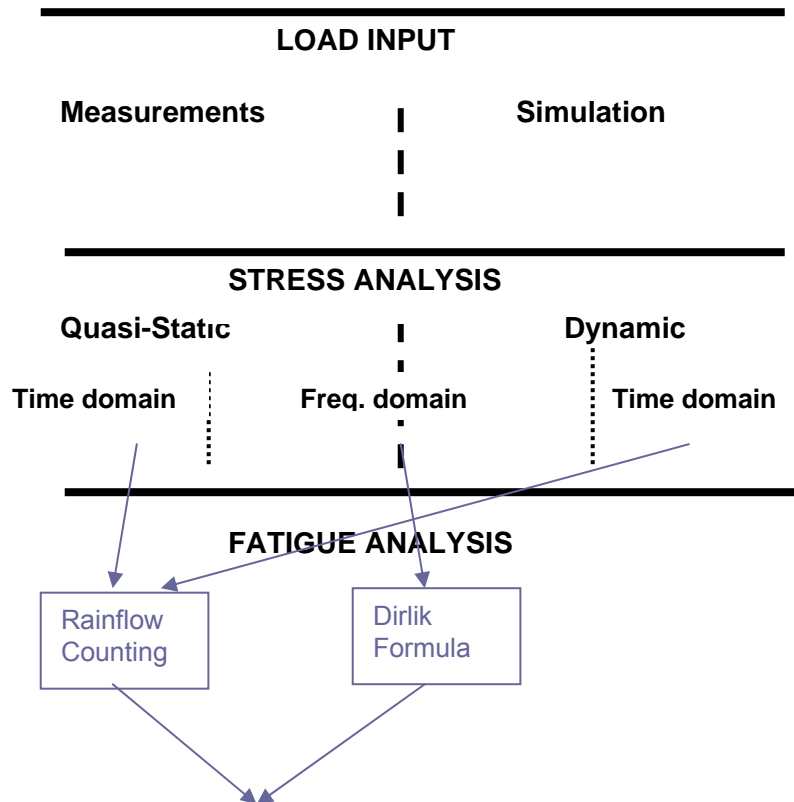


Figure 3-12 Cycle Counting Methods

The second requirement implies the obvious condition in that it is imperative to know the factor by which a test is accelerated, should accelerated testing be performed. The added complication is that the acceleration factor must be known for all possible modes of failure (an accelerated test in terms of vibration loads would for example achieve different acceleration factors for mechanical components than for electronic components).

The third requirement implies that it is necessary to employ a statistical approach to be able to take account of statistical variables which could influence the performance of the system. This becomes necessary since it is obviously only possible to perform durability tests on a sample population.

The development of a testing methodology that would conform to the above validity requirements is logically set out in Table 3-2. Different levels of testing are logically developed. The lowest level test involves the idealized case where the total population of fully assembled systems are tested for the total lifetime, being subjected to all loading conditions experienced during service.

In order to develop a practical test (on a higher level of sophistication), certain technical aspects need to be addressed, as listed in the last row of the table. The optimal level of testing may be derived by balancing the cost of testing (a low level test implies a high cost due to large samples, long durations and comprehensive simulation of loading conditions) and the cost of developing a higher level of testing (the expertise required to address the technical aspects is costly).

For each higher level of testing all technical considerations listed at the lower levels need to be addressed.

**Table 3-2 Levels of durability testing**

Level	0	1	2	3	4
<b>Assembly level</b>	Complete system	Complete system	Complete system	Complete system	Component level
<b>Acceleration</b>	None	None	None	Accelerate	Accelerate
<b>Sampling</b>	Total population	Large sample	Limited sample	Limited sample	Limited sample
<b>Comprehensiveness of loading</b>	Comprehensive	Comprehensive	Reduced Inputs	Reduced inputs	Reduced inputs
<b>Application method</b>	Actual service	Simulate	Simulate	Simulate	Simulate/ single amplitude
<b>Technical considerations</b>	None	What to simulate? How to simulate? Statistics	Insignificant inputs? Statistics of limited samples	Acceleration factors?	Interaction effects?

The technical considerations listed in the above table are individually dealt with in the following paragraphs:

- **Mission profile**  
In order to design a lifetime test it is imperative to detail the mission profile of the system in terms of all loading conditions. These include consideration of operational modes, operational life, external inputs, environmental conditions, operator influence and others. No valid test method could be developed without establishing the mission profile.
- **Simulation methods**  
Methods to simulate all loading conditions must be designed. Lower level testing involves true laboratory simulation of actual loading conditions. Simulation of vibration inputs typically requires that acceleration measurements be performed on an actual system in service, which could then be reconstructed in the laboratory.

For higher level testing, simulation of actual (random) loading conditions may be replaced with idealized simulation such as block loading or single amplitude loading. In this case it is necessary to determine the damage content of the idealized loading in terms of the actual loading conditions. It is therefore required to develop failure models for all possible failure modes.

- **Insignificant inputs**  
Simulation of all loading conditions could be severely restrictive in terms of economic viability. It is therefore necessary to identify insignificant loading conditions. This will require that all possible failure modes be identified and that failure models of all modes should be established. These failure models would involve mathematical expressions of life to failure in terms of loading parameters.
- **Acceleration**  
Required operational life would typically imply impractical testing durations. It is therefore necessary to accelerate the test. Acceleration is achieved by testing under more severe conditions to what would be expected in service, i.e. test with higher loads. In order for the test to be valid, it is necessary to establish the factor with which the test is accelerated. Typically, a power law (for fatigue failure) or inverse power law (for bearing failure) failure model is assumed. With knowledge of the failure model constants, it is then possible to relate the expected service life under normal loading to the test life under increased loading.

It is therefore imperative to derive failure models for all possible failure modes in order to be able to accelerate the reliability testing. Acceleration of all failure modes would not be achieved equally by increasing certain loads. It is therefore possible that failure modes being dominant under actual service loading would not be dominant under increased loading conditions. The only way by which to address this problem would be to model all failure modes.

Accelerated testing on component level would be considerably easier than full system testing since each component could be tested with different acceleration factors. It may not be possible to achieve uniform accelerated complete system testing. It may therefore be optimal to perform component level accelerated testing in conjunction with complete system testing (partially accelerated).

- **Statistics**  
Well established statistical methods exist to derive reliability data from test results. Classical statistics require a large number of specimens to be tested to enable practical confidence levels to be achieved. The next section deals with the viability of inferring practical reliability data from small sample testing. A more fundamental problem is however the fact that reliability data for the product must be inferred from testing only a sample of the total population, be it a large or a small sample, whilst it is, due to the complexity of the system, difficult to prove that all influences on the system have been taken into account in the reliability formulation.
- **Statistics of limited sample testing**  
It is possible to infer reliability data from limited sample testing using Bayesian Inference. The principle behind this method is that if prior knowledge of the expected distribution is obtained, fewer specimens are required to achieve practical confidence levels. It is therefore again necessary to establish failure models for all failure modes.
- **Interaction**  
When component testing is performed it will be necessary to determine loading conditions for each component. Therefore it is required to analyse the interaction between the different components of the system.

Comments from the literature concerning the above aspects are discussed in detail in the following sections.

#### 3.4.6.1.2 Process

The purpose of durability testing is to determine the life to failure of the structure in terms of some measure of customer usage. According to Leese and Mullin (1991), many companies have spent decades relating (correlating) their proving grounds with typical customer service usage. This process is one of the main themes of the present study. If it is assumed that this work has already been done, the purpose of correlation is to ensure that any test method used, represents the same severity of testing than would the defined proving ground test sequence. This is mostly done in terms of fatigue damage. Leese and Mullin (1991) describe the process of performing fatigue calculations to correlate proving ground to proving ground, proving ground to laboratory test and test to test.

#### 3.4.6.1.3 Acceleration factor

Two important concepts need further discussion. The obvious intention of laboratory testing is to accelerate the test in comparison with the proving ground test. This is already achieved through the fact the test rig could run for 24 hours per day. Additionally, however, the non-damaging sections of the proving ground test sequence may be edited out of the laboratory test sequence. These will obviously include sections which are unavoidable on a physical track such as turn-around spaces.

Proving grounds are usually already accelerated in relation to average customer usage (typically by a severity ratio of 5 – 10). It is normally possible to achieve a further compounding severity ratio in the laboratory of 2 – 5. Mathematically it is possible to accelerate testing almost by an unlimited factor by increasing the amplitudes of the stresses. This is sometimes done by multiplying the measured signals with a factor larger than one and then to apply drive signals to achieve this on the rig. This practice is

however not desirable, since it may imply a different failure mechanism to come into play, such as low cycle fatigue. Barton (1991) describes a method to minimize the maximum test stress whilst achieving the desired acceleration factor.

#### 3.4.6.1.4 Equalised acceleration

Secondly, the requirement to achieve equal acceleration of all reference channels, may be commented on. If unequal acceleration is applied, it would mean that some parts of the structure would be tested faster than others. An example of this may be when a channel on a suspension component sensitive to braking wheel forces is less accelerated to a channel sensitive to vertical wheel forces on a four poster test rig, due to the fact that braking forces are not simulated on the rig. It is then obvious that such a test would not prove the integrity of the former component.

A further example may be a channel on a chassis crossmember sensitive to twisting of the chassis, compared to a bending gauge on the chassis beam, sensitive to vertical bending. In such a case, it will be possible, for instance, to include a correct mix of out-of-phase and in-phase sections in the final sequence. An algorithm to derive the optimal sequence in terms of equal and maximized acceleration was developed during a post-graduate study, supervised by the present author and is reported on by Niemand (1996). This process is also followed when designing a sequence on the proving ground to simulate customer usage.

The process of establishing an optimal test sequence with equalized acceleration for all channels, presents a very non-linear problem, as recognized by Moon (1997), where the application of neural networks in the development of testing sequences, is described.

#### 3.4.6.1.5 Choice of fatigue exponent

It is important to note that, when using the stress-life approach, only the fatigue exponent ( $b$ ) would influence relative fatigue calculations, since the fatigue coefficient, as well as other factors, such as stress concentration factors, would divide out. The calculation of a durability test severity ratio (or acceleration factor) would give different results with different  $b$ -values. This would be true for any accelerated test (levels 3 or 4), be it using simulated loading, block loading, or single amplitude loading.

It follows that it is of importance to choose the correct value for  $b$  when such relative damage calculations are performed (Niemand (1996)).  $b$  may typically vary between  $-0.05$  for some parent metals, to  $-0.333$  for welds in steel or aluminium (Olofsson et al. (1995)). A value between  $-0.25$  and  $-0.3$  is typical for failure of non-welded metal with significant stress concentrations. A value of  $-0.333$  is normally chosen when weld failures are expected, otherwise a value of  $-0.25$  or  $-0.27$  is often used.

For a component test, the problem may not be relevant, since the component could have a single fatigue exponent (i.e. be of an homogeneous material, without welding). For component or assembly testing, where different fatigue exponents are relevant, it has to be accepted that different severity ratios will be achieved during a test for different details of the assembly or component.

The same considerations with regard to the choice of fatigue exponent also exist for all the analysis (as opposed to testing) methods employed during the present study.

Equivalent to testing methods, analysis methods also require input loading (in the case of analysis methods, being input loading for e.g. finite element analysis rather than for a physical test on a component or assembly), that is representative of in-service loading conditions by some fatigue damage ratio (e.g. five minutes of dynamic finite element analysis stress results represents the damage of one hour of real life). Again this ratio will be mathematically dependent on the fatigue exponent used for the damage calculations.

#### 3.4.6.1.6 Synthetic test signals

The above paragraphs have concentrated on laboratory tests where the measured response on the proving ground is simulated in the laboratory. In terms of fatigue damage, the same calculation principles will also apply when using synthetic test signals, such as constant amplitude or block loading signals. A method is described by Lin and Fei (1991) to use a progressive stress (stress increasing over time) approach for accelerated testing.

#### 3.4.6.1.7 Testing for modes of failure other than fatigue

Testing for wear, corrosion, lubrication failure, electronic component failure, rattle-and-squeak and many others, also require methods to accelerate the testing, whilst quantifying the relation between the laboratory test and real life.

Energy content is used for calculating acceleration for rattle-and squeak tests (Hurd (1992)). Moura (1992) describes temperature accelerated testing on electronic components, using the Arrhenius equation, which is similar to the stress-life equation, with temperature instead of stress.

Accelerated corrosion testing presents large difficulties and is not dealt with in the present study.

#### **3.4.6.2 Laboratory load reconstruction**

A laboratory test method, employed for both the minibus and the pick-up truck case studies, involves the accurate simulation in the laboratory of loads measured on a test track or road. The testing was performed under the supervision of the present author, by the Laboratory for Advanced Engineering (Pty) Ltd. The specialized mathematical technique required for this load reconstruction is described by Raath (1997).

Specialised software (Qantim™) was used for the calculation of the drive signals for the test rig, such that the remotely measured responses are accurately simulated. The basic steps utilised in this technique are briefly outlined below:

- The test rig is excited with a pseudo random white noise, while simultaneously recording all relevant responses (accelerations or strains). As many responses as there are drive actuators, are required. They are normally carefully chosen so as to be each sensitive to only one drive force, thereby limiting the cross influence.
- A time-domain based dynamic model is found from the input-output data using dynamic system identification techniques. This model is identified in the reverse sense, i.e. output response multiplied by dynamic transfer function yield random input.
- The transfer function is then used to calculate the actuator input signals from the desired measured response signals.

- The actuator input signals are then applied to the test rig, while recording the achieved response signals.
- By comparing the desired and the achieved responses, response errors are found, which are again simulated using the transfer function, to give the error in the actuator input signals. The input signals are then updated to give the new input signals.
- The above procedure is repeated until the achieved response signals match the desired response signals.

An equivalent method in the frequency domain, called Remote Parameter Control (RPC) is described by Dodds (1973). Dong (1995) describes a method using time domain series models, without the need for sophisticated software systems.

#### **3.4.6.3 Synthetic signal laboratory testing**

The testing of bus structures using synthetic laboratory signals, such as block loading and constant amplitude loads, is described by Kepka and Rehor (1993).

### **3.4.7 Statistical Analysis**

#### **3.4.7.1 Cause and effect of variations in fatigue testing results**

Cutler (1998) discusses the cause and effects of variations in fatigue testing results. It is argued that the cause of variations in fatigue results should be investigated and where appropriate be linked to particular aspects, such as measurements, methods, machines, environment, people or materials. Plots of residuals against fits need to be checked for structure, trends or serial correlation.

#### **3.4.7.2 Bayesian Inference**

A method is described by Giuntini (1991) that enables true failure data to be combined with prior predictions to yield a posterior estimate of a failure distribution. This method is of importance, since with structural durability testing, it is often not possible to perform a sufficient number of tests to obtain a statistically significant sample, whereas years of experience with similar components do provide significant prior knowledge.

The method requires a choice of distribution, as well as an estimate of the parameters defining the prior distribution. The real failure data is then used to fit a failure distribution. Random samples are generated from these two distributions using the Monte Carlo method. The samples are combined according to a chosen proportion (indicating the user's relative confidence in the two prior distributions), which are then used to fit a posterior distribution. The method was employed during the pick-up truck case study presented later and also discussed by Slavik and Wannenburg (1998).

#### **3.4.7.3 Statistical correlation between usage profile and durability test**

A statistical methodology to establish the correlation between the usage profile and the durability test, is described by Beamgard et al. (1979). The methodology consists of a user survey, where information pertaining to cargo transported, annual vehicle mileage, as well as percentages of mileage driven on various categories of public roads are gathered, a measurement phase, where fatigue damage induced by the various categories of roads are quantified, as well as a statistical analysis using the Monte Carlo method, where the statistical correlation is derived.



The result is shown in the form of a graph of customer distance vs durability distance (severity ratio) for various percentile customers. It is argued that verification of the method against field failure data is imperative. It is also argued that, for such verification to be accurate, it is important to determine the mortality of vehicles for reasons other than structural failures. Such data is given by Liberty (1993). A methodology similar to the above was employed for the minibus, as well as the pick-up truck case studies.

### 3.5 DETERMINATION OF INPUT LOADING

#### 3.5.1 General

According to Grubisic (1994), the service life of a vehicle component depends decisively on the loading conditions in service. It is necessary that a representative loading spectrum is defined for both design and testing purposes. If not, the most sophisticated analysis or testing techniques will yield no useful results. In this section, some important current practices in this regard are described.

#### 3.5.2 Sources and Classification of Loading

The contents of this and the following two sub-sections, are mainly taken from the paper by Grubisic, with some additions by the present author.

It is argued that the main influencing parameters on the loading spectrum may be defined as *usage* (vehicle utilization and driver), *structural behaviour* (vehicle dynamic properties and the design) and *operational conditions* (quality and type of road). This definition is similar to that used by Slavik and Wannenburg, where the terms *usage*, subdivided into *magnitude* (driver influence and vehicle utilization, e.g. distance per month) and *severity* (operational conditions), were used, together with the term *durability* (vehicle properties from design and manufacture).

It is also argued that the importance of the component under consideration needs to be taken into account. Primary components, subdivided into safety critical component and functional components, as well as secondary components are defined.

Loads originate from road roughness (strongly influenced by speed), manoeuvres (braking, accelerating, steering), power generation (engine), transmission, cargo/passenger interaction with structure, wind, accidental impact loads, as well as events such as driving over a curb.

Loads may be classified as (quasi-)static versus dynamic, random versus deterministic, transient (as in the case of events) versus stationary, fatigue versus overload, etc.

Consideration of both the sources and the classifications is important, as it facilitates better understanding, comprehensiveness and correct treatment.

As all structures represent more or less complicated elastic systems, time varying operational loads could excite natural modes. Stress response at a certain location on the structure will therefore show the effect of both the input loads, as well as the dynamic characteristics of the structure.

### 3.5.3 Design Load Spectrum

Most load histories are random in nature, implying the use of statistical functions which allow the derivation for the occurrence of certain values. Most methods to derive these statistical functions (generically called cycle counting methods, which included rainflow counting, PSDs etc.) are one-dimensional, i.e. only magnitude and number of occurrences are counted. Any such result may therefore be defined as a load spectrum (magnitude versus cumulative frequency).

The main parameters of the arguments of Grubisic are depicted in Figure 3-13, which is somewhat adapted from the reference by the present author. The characteristics of both the loading, as well as the material fatigue properties could be represented on a log-log plot of stress amplitude versus number of cycles. The loading, thus represented is the load spectrum, where-as the material properties are presented as SN-curves.

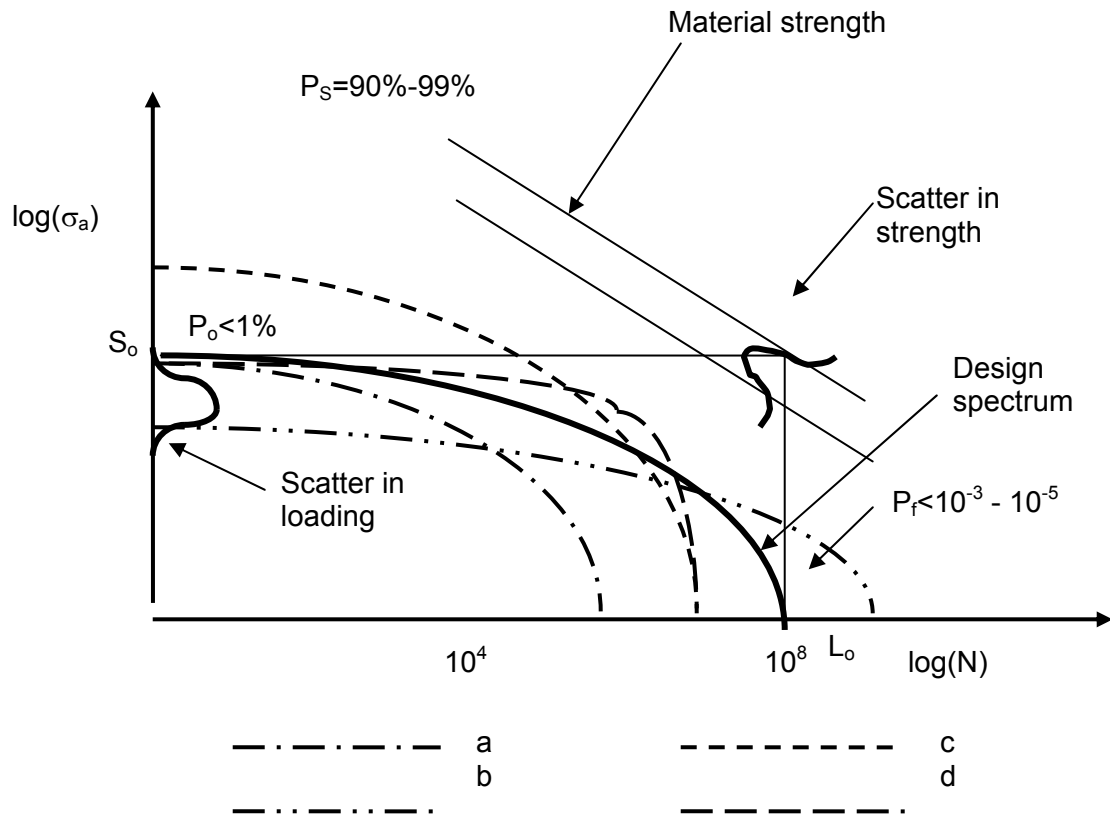


**Figure 3-13 Load spectrum diagram (Grubisic)**

Load spectrum curve [a] may for argument sake represent the loading on an automotive component in off-road conditions (high amplitudes, low number of cycles), where-as curve [b] may represent the same component loading under highway loading conditions (low amplitudes, high number of cycles). The two together and others in between represent the scatter in loading on a component.

From these, a design spectrum with a probability of occurrence of typically less than 1 %, must be defined, resulting in a probability of failure (which needs to be calculated taking into account the scatter in material strength and taking a 90 % survival probability for initiation and 99 % for fracture) of typically  $10^{-3}$  to  $10^{-5}$ .

Additional to the design spectrum, for some components it is necessary to take into account individual unexpected overloads coming from special events such as accidents. These loadings are predominantly impact loads and do not influence the fatigue behaviour.

The loading design spectra must be determined from measurements, taking into account different operational loading conditions (cornering, bad surface, straight driving, braking & acceleration, etc.), as well as customer usage. Strategies to quantify the latter may involve measurements with vehicles driven by several different test drivers over different road segments, measurements on a test vehicle following customer vehicles, or simple measurement devices installed on customer vehicles. In the present study, several detailed procedures for quantifying customer usage, are presented.

#### **3.5.4 Test Load Spectrum**

Methods for the derivation of test spectra are also presented by Grubisic. A test program should assure a reliable approval of the expected service life and have the highest possible acceleration to minimise test time and cost. The following possibilities to achieve this are listed:

- Increase the test load frequency. This may be used in uni-axial tests, where the testing frequency is not exciting any natural frequencies of the component.
- Increase the maximum load amplitudes (see curve [c] in Figure 3-13). This method has the danger of causing other failure mechanisms, such as plastic deformation, to come into play and is therefore normally avoided.
- Omit low non-damaging loads. Typically the level of omission would be at between 0.2 and 0.4 of the maximum loads.
- Do not exceed maximum load amplitudes, but increase other load amplitudes and omit non-damaging loads (see curve [d] in Figure 3-13). Typically, for a vehicle suspension component, achieving more than 100 million cycles in its life, a durability test would have between 2 million and 7 million cycles at similar frequencies, implying an acceleration factor of around 30.

#### **3.5.5 Road Roughness as a Source of Vehicle Input Loading**

It is recognized that road roughness plays a significant role as a source of vehicle input loading. From a pavement engineering point of view, substantial research has been conducted to establish measurable parameters to quantify road roughness (as quality and maintenance criteria). A method to predict vertical acceleration in vehicles through road roughness is described by Marcondes and Singh (1992). The method uses the International Roughness Index (IRI), together with dynamic characteristics of the vehicle, to predict the PSD of vertical acceleration of the vehicle.

The present author initiated a study, with the purpose to use the IRI to classify road types for durability requirement establishment. It was argued that the existing classifications, e.g. highway, secondary tar, gravel, etc., leave room for misinterpretation between questionnaire participants during user surveys and measurement engineers. The results of the study are presented by Blom and Wannenburg (2000).

The IRI statistic of a specific profile section is determined by accumulating the measured suspension motion linearly and dividing the result by the length (L) of the profile section.

$$IRI = \frac{1}{L} \int_0^{L/v} |\dot{x}_s - \dot{x}_u| dt$$

with

$v$  = speed over section

$\dot{x}_s$  = vertical velocity of sprung mass

$\dot{x}_u$  = vertical velocity of unsprung mass

### Eq. 3-24

The IRI value ranges from 0 (for totally smooth surface), through to 30 (for unpaved section traversable only at slow speeds). The strength of the method is that descriptive road classifications may be coupled to an IRI value (see Table 3-3). The correspondence between subjective classifications (by a range of typical vehicle users) and measured IRI values is depicted in Figure 3-14. A bias towards overestimating the IRI value for higher value roads, was observed. This would indicate that the descriptive classifications may need to be adjusted somewhat.

The correspondence between the measured IRI and the calculated relative fatigue damage is depicted in Figure 3-15. On a log-log plot, there is a linear relationship with a gradient approximately equal to the fatigue exponent used for the fatigue calculation. This result is interesting from the following perspectives:

- It indicates the viability of deriving fatigue loading from IRI data (since it is possible to derive PSD data from IRI values - Marcondes and Singh (1992) - and fatigue loading from PSDs - Sherratt (1996)), this result is to be expected.
- It shows the importance of correct estimation of usage of higher IRI valued roads, since there is a highly non-linear (power law) relationship between the IRI value and the fatigue damage.

The principle of using a roughness index to categorize roads for usage profiles is also discussed by Blom and Wannenburg.

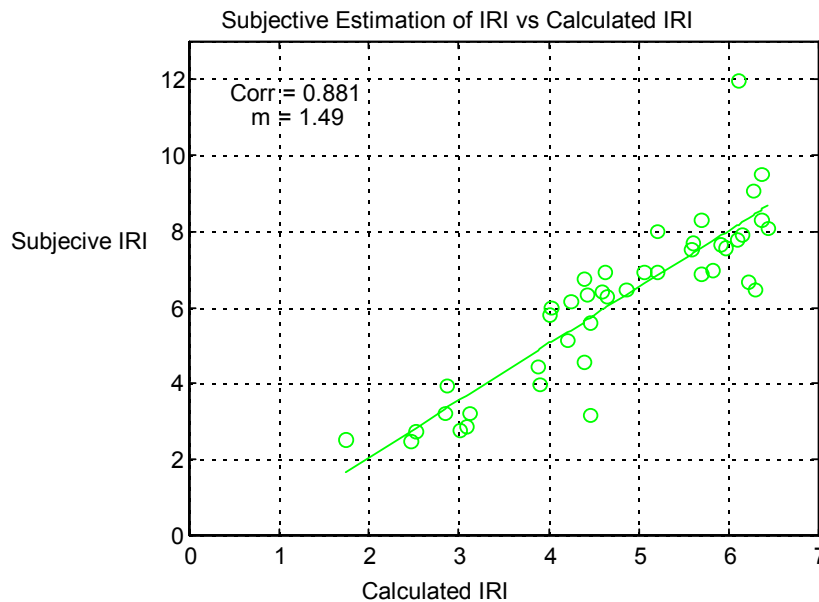


**Figure 3-14 Subjective IRI vs calculated IRI (from Blom and Wannenburg)**

**Table 3-3 (from Blom and Wannenburg) Road classifications for subjective IRI**

Description	IRI
<b>Paved Roads</b>	
A comfortable ride perception is obtained at speeds equal to or greater than 120km/h. No depressions, potholes or corrugations are noticeable. Surfaces with undulations are barely perceptible at a speed of 80 km/h with the roughness ranging from 1.3 to 1.4. High quality highway surface 1.4 to 2.3 and high quality surface treatment sections 2.0 to 3.0.	0 - 2
A comfortable ride perception is obtained at speeds up to 100-120km/h. Moderate perceptible movements or large undulations may be experienced at 80km/h on surfaces displaying no defects. Occasional depressions, patches or many shallow potholes are descriptive of a defective surface.	2 - 5
A comfortable ride perception is obtained at speeds up to 70-90km/h. Profound movements and swaying are perceived on surfaces with strong undulations or corrugations. Frequent moderate and uneven depressions or patches, or occasional potholes.	5 - 8
A comfortable ride perception is obtained at speeds up to 50-60 km/h. Frequent sharp movements and/or swaying associated with severe surface defects. Frequent deep and uneven depressions and patches, or frequent potholes.	8 - 10
It is inevitable to reduce speed to below 50 km/h. Surfaces display many deep depressions, potholes and severe disintegration.	10 - 12
<b>Unpaved Roads</b>	
Recently bladed surface of fine gravel, or soil surface with excellent longitudinal and transverse profile (usually found only in short lengths). A comfortable ride perception is obtained at speeds up to 80-100km/h. The awareness of gentle undulations or swaying.	0 - 6
A comfortable ride perception is obtained at speeds up to 70-80 km/h. An awareness of sharp movements and some wheel bounce. Frequent shallow-moderate depressions or shallow potholes. Moderate corrugations.	6 - 12
A comfortable ride perception is obtained at a speed of 50 km/h. Frequent moderate transverse depressions or occasional deep depressions or potholes. Strong corrugations.	12 - 16
A comfortable ride perception is obtained at 30-40 km/h. Frequent deep transverse depressions and/or potholes or occasional very deep depressions with other shallow depressions. Not possible to avoid all the depressions except the worst.	16 - 20
A comfortable ride perception is obtained at 20-30 km/h. Speeds higher than 40-50 km/h would cause extreme discomfort, and possible damage to the vehicle. On a good general profile: frequent deep depressions and/or potholes and occasional very deep depressions. On a poor general profile: frequent moderate defects and depressions.	20 - 24

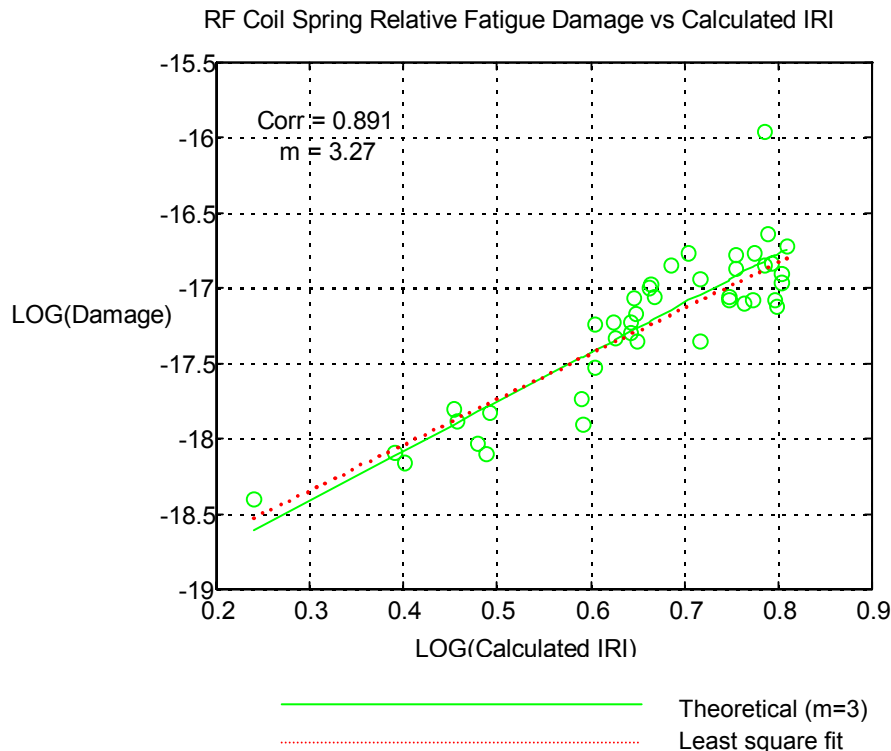


**Figure 3-15 (from Blom and Wannenburg) Fatigue damage vs IRI**

The results of this study were unfortunately not available at the time when the two relevant case studies (minibus and pick-up truck) were performed (the study was initiated by the author as a result of the work performed during the case studies). The more scientific road classification approach was therefore not incorporated at the time, but the developed method is proposed as part of the generalized methodology presented in Chapter 1.

### 3.5.6 Vibration

Richards (1990) presents a review of analysis and assessment methodologies for vibration and shock data to derive test severities, mainly for the transport industry. The following general observations are of importance:

- A significant proportion of the dynamic environment experienced by cargo on vehicles originates from the interaction between road wheels and road surface. This is fundamental to much of the work presented in the present study.
- Vehicle speed is one of the major influencing factors on the severity of vibrations.
- The vibration dynamics contain both continuous and transient responses, which are often difficult to separate, due to the irregularity of the transient occurrence intervals and amplitudes. Continuous response is traditionally termed vibration and the transient response is considered as shocks. These factors played a major role in the tank container case study presented later.

Four methods to determine vibration test severity are reviewed by Richards:

- PSD approach: The test severity is derived from the Power Spectral Density of measurements. The limitation of this method is that, due to the averaging, transient events and time varying data (non-stationary) cannot be described.
- Sandia approach: Based on comprehensive measurements, the most severe values of root-mean-square acceleration for each of several frequency bandwidths, are derived.
- Aberdeen Proving Ground approach: The method uses the mean acceleration PSD values using a 1 Hz bandwidth, along with the standard deviation in each band. One standard deviation is added to the mean to provide a testing envelope. The method can be distorted when non-stationary data is used. Measurements on a test track should therefore happen at constant vehicle speed over each section.
- Cranfield approach: The method included both the acceleration PSD and the Amplitude Probability Density Function (APD). The PSD gives the spectral shape, but the overall amplitude is modified using the APD. Transient events are thus included as short duration, high amplitude, random vibration.

To some extent the method used for the tank container case study, is similar to the latter approach. The tank container case study is interesting in the sense that it could be regarded as cargo being transported on vehicle (falling into the regime described in this section, namely so-called vibration testing), or can be seen as a vehicle structure in itself, where fatigue based methods are more commonly employed. The statement is made by Devlukia (1985) that PSDs and APDs are not sufficient to establish fatigue loading characteristics, advocating the use of rainflow counting.

A European research project, to establish an integrated system for the design of vibration testing, is described by Grzeskowiak et al. (1992). This process is called 'tailoring', a term used by vibration testing engineers. It would seem that fatigue domain analysis is recognized in this project. The present study, to a large extent, is aimed at the same objective.

### 3.5.7 Limit State and Operational State

In principle the process for static design is simple. Structural response (stresses, displacements, etc.) to some defined input loading is determined, either through analytical calculations, or finite element methods. These results are then evaluated against a set criterion for allowable quantities. The allowable quantities would be material property related (e.g. yield stress) or functional (e.g. maximum allowable displacements).

Traditionally, a strength design criterion is set in the following format;

$$\begin{aligned} & \text{Calculated maximum stress (function of defined loading \& geometry)} \\ & < \\ & \text{Allowable stress,} \end{aligned}$$

where the allowable stress would be a material strength (e.g. yield stress) divided by a safety factor. The safety factor may then typically take the following into account:

- Uncertainty with regards to the material strength.
- Uncertainty with regards to the loading.
- Dynamic loading effects.

- Fatigue loading effects.
- Stress concentrations, welding etc.

In some cases, design criteria are set which incorporates an obvious safety factor on the prescribed loading, as well as an additional safety factor applied to the material strength. Such safety factors should rather be called factors of ignorance, since they attempt to take account of aspects not quantified scientifically.

A more logical approach, called the limit state design method MacGinley and Ang (1992), requires the designer to define limit states and operational states. Much smaller safety factors are then prescribed to allow mainly for statistical uncertainty of material properties. As an example, a designer of a tanker truck would then have to define the following limit states:

- Maximum vertical, lateral, longitudinal (separate and/or combined) loading for no damage to vehicle. Here travelling over a hump in the road at a high speed with a full load, may define the maximum vertical load. The maximum longitudinal load may be during maximum braking effort under full load and the lateral load could be during a high speed double lane-change manoeuvre, or during a scuffing event on a concrete tarmac.
- Maximum longitudinal load for no leaking of tank. This may be some accident situation, where the truck collides with another vehicle.
- Fatigue limit state loads, where vertical, longitudinal and lateral load amplitudes, as well as repetitions during the design life of the vehicle, need to be defined.
- Other limit states, such as energy to be absorbed during a roll-over without the tank leaking, penetration damage to the tank vessel, energy to be absorbed by bumpers and underrun bars during accidents.

With the responsibility of defining these design limit states being put on the designer, there is then no need for applying safety factors on the loads to be used in the design, but it does put an added responsibility on the design engineers.

In many industries, however, the more traditional approach is still adhered to in design codes. In the road tanker industry, a South African design code, SABS 1398 (1994), defines the following design criteria:

Maximum principal stresses calculated for the following separate loading conditions shall be less than 20% of the ultimate tensile strength of the material:

- Vertical load = 2 g
- Longitudinal load = 2 g
- Lateral load = 1 g

Since a 2 g longitudinal acceleration cannot even be approximated during hard braking and a 1 g lateral acceleration would overturn most road tankers, it is obvious that safety factors are applied to the loading side of the static design equation. Also, an additional safety factor of 5 is enforced on the material strength.

An equivalent American design code, Code of Federal Regulations, Title 49, requires that the maximum principal stresses calculated for the following combined loading condition shall be less than 25% of the ultimate tensile strength of the material:

- Vertical load = 1.7 g



- Longitudinal load = 0.75 g
- Lateral load = 0.4 g

In this case, the loads seem much closer to realistic limit state loads, but the safety factor of 4 on the material strength must involve more than just allowance for scatter in material properties. Both these codes do not prescribe any fatigue loading and it is therefore apparent that the safety factors incorporate allowance for fatigue.

A further factor contributing to the high safety factors in these codes is the fact that they assume very simple hand calculations to be performed, resulting in only global bending, tensile and shear stresses caused by the prescribed loads and not peak stresses at stress concentrations, such as will result from detailed finite element analysis. It would therefore be erroneous to evaluate localized high finite element peak stress results using such codes without further interpretation.

In the USA Federal Regulations code for the design of ISO tank containers, a criterion is prescribed for stresses resulting from a combined;

- Vertical load = 3 g,
- Longitudinal load = 2 g,
- Lateral load = 1 g,

to be lower than 80% of the yield stress of the material. When applying these loads to a detailed finite element model, it is doubtful whether any design in the world strictly complies.

Sophisticated design codes, such as the ASME code for pressure vessels, allow for the interpretation of detailed finite element stress results, where allowable local stresses can be more than twice the yield strength of the material, based on the fact that local yielding would occur with the resultant redistribution of stresses. Such peak stresses would therefore not be detrimental to the static integrity of the structure, but under repetitive or variable loading (to which vehicle structures are subjected), such areas would be of high concern for fatigue problems.

### **3.5.8 Design and Testing Criteria**

#### **3.5.8.1 Maximum load criteria**

##### **3.5.8.1.1 Automotive vehicles**

A design criterion in terms of static inertial loads is described by Skattum et al. (1975).

- Vertical load = 3 g
- Longitudinal load = 2 g
- Lateral load = 1 g

The vertical load is substantiated from measurements, where it was found that a 3 g vertical load would be exceeded with a 3% probability.

Riedl (1998) describes an exercise to substantiate the design of aluminium components of the BMW 5-series rear axle, with particular consideration of extreme loads. Testing was performed using pendulum induced impact loads.

### **3.5.8.2 Fatigue loading**

#### 3.5.8.2.1 Inertial Loading

As discussed in paragraphs 3.5.7 and 3.5.8.1.1 above, it is typical to find loading criteria for automotive structures in design codes expressed in terms of inertial loading (also called g-loading). As argued in paragraph 3.5.7, it would seem that such criteria would often also make allowance for fatigue loading.

The obvious reason for using inertial loading in design criteria, is that inertial loading may be generic (independent of specific design, or more specifically, the specific design mass). Since it is a principal objective of the present study to establish fatigue loading design criteria for automotive and transport structures, a methodology was developed based on fatigue equivalent static g-loading.

Xu (1998) argues that g-loads are sufficient to capture the structural response to the three principal global loading modes experienced by vehicles, namely, bouncing (vertical g-load), pitching (longitudinal g-load) and rolling (lateral g-load). Xu introduces the concept of modal scaling to supplement the quasi-static g-loads, which would be able to address response modes beyond these three. The method is in principle equivalent to the modal superposition method discussed in paragraph 0. For the LTV case study, it was required to employ a hybrid g-loading / modal superposition method similar to that described by Xu.

#### 3.5.8.2.2 Remote Parameter Analysis

A concept termed Remote Parameter Analysis (RPA), developed at Ford Motor Co. to integrate finite element analysis and simulation or road test data for durability life prediction, is described by Pountney and Dakin (1992). The method is of importance since it allows component optimisation earlier in the design process, due to the ability to derive free-body component forces from measurements on customer correlated routes. Since a finite element simulation process is some 30 times faster than laboratory simulation and some 90 times faster than proving ground simulation, the period of time spent in the design and development phases can be significantly reduced.

The method involves the following steps:

- Develop a free body diagram of the component under consideration.
- Construct a finite element model of the component.
- Select a constraint set and apply unit loads to the finite element model.
- Derive from the results, a load-to-gauge transfer matrix, taking care to choose the positions of the strain gauges such that effective decomposition is achieved. The inverse of this matrix is used to determine the loads acting on the component from the time data measured at the strain gauges.
- Derive also a load-to-response transfer matrix. This matrix enables very fast solution of the stresses on the component for each time step load set solved during the previous step, without having to perform the finite element analysis again.
- Fatigue analysis on the stress-time result at any position on the component can then be performed.

The method is based on static linear models, therefore disregarding the effect of dynamics (i.e. it is a quasi-static method). Poutney and Dakin state that most

engineering problems can however be solved using the static linear models. The majority of the methods employed in the present study are also based on this important simplifying assumption.

The RPA methodology is essentially an extension of the quasi-static method depicted in Figure 3-2. The RPA method is depicted on the summary diagram in Figure 3-16.

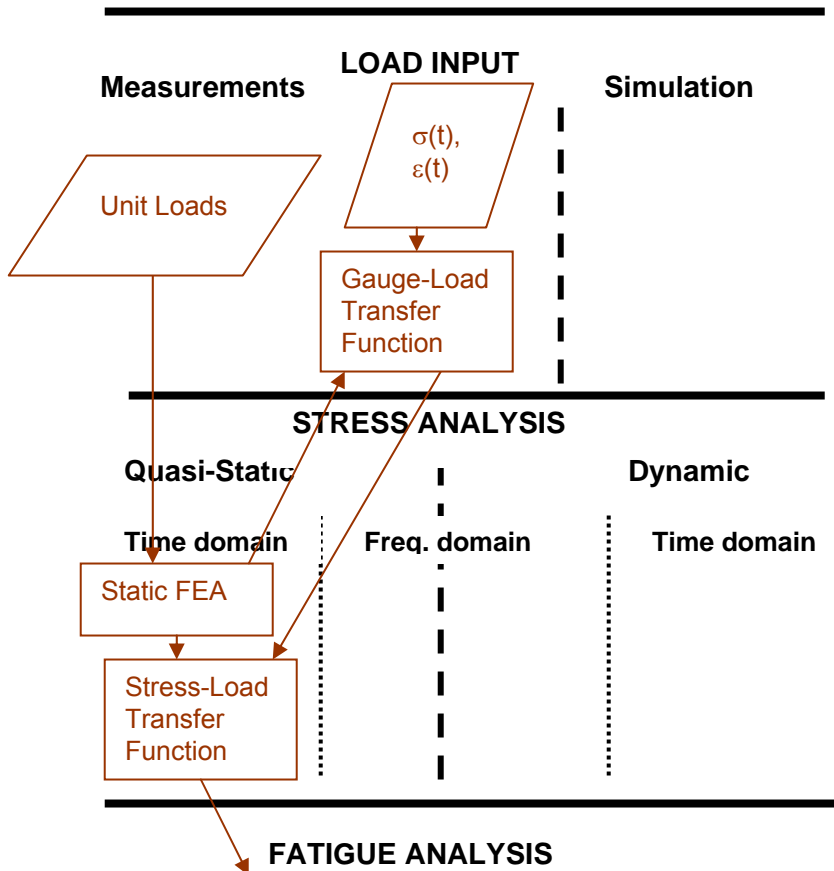


**Figure 3-16 Remote Parameter Analysis**

A fully dynamic method with similar steps may be derived from the mathematical process used to reconstruct real road input loading in the laboratory from remotely measured parameters such as strains, according to Raath (1997). Here the laboratory rig would be substituted by a dynamic finite element model, where time-domain or frequency domain transfer functions between dynamic identification input loads and dynamic responses at measuring positions are fitted on the finite element results, to be able to derive dynamic input loads (simulating the real loads) for dynamic finite element analysis.

#### 3.5.8.2.3 Standardised load-time histories

Heuler et al. (2005) reviews a large number of Standardised Load Time Histories (SLH) developed over 30 years in the aircraft (e.g. FALSTAFF, Gerharz (1987)) and automotive industries. Such systems are the result of collaborative efforts by industry working groups and typically involve comprehensive measurement exercises, the results of which are statistically processed to obtain standardised load spectra. One such

system, named CARLOS (Schutz et al. (1990)), produced vertical, longitudinal and lateral random load sequences, being a mixture of 5 road types, which are used for front suspension durability testing.

#### 3.5.8.2.4 Statistical domain

A statistical model of random vehicle loading histories is described by Leser et al. (1994). The load history is considered to have stationary random and non-stationary mean contents. The stationary variations are modelled using the Autoregressive Moving Average Model (ARMA), while a Fourier series is used to model the variation of the mean. The method enables the construction of time domain data for analysis or testing purposes.

#### 3.5.8.2.5 Frequency domain

A novel approach to establish fatigue loading for road tankers is presented by Olofsson et al. (1995). A survey of more than 1000 gasoline road tankers in Sweden found that more than 40 % of the vehicles were impaired by cracks caused by fatigue, indicating that the existing design criteria are insufficient to guard against fatigue failure. The method is based on an extension of the Shock Response Spectrum (SRS) approach, commonly used to described shock loading (e.g. for earthquake analysis). The approach is called the Fatigue Damage Response Spectrum (FDRS) and is used in France to create fatigue test sequences for structures. The process to establish a FDRS can be summarized as follows:

- From measured acceleration data the response of a single degree of freedom dynamic system with varying dynamic properties (natural frequency and damping) is determined using FFT analysis.
- For each response, the fatigue damage is calculated using the stress-life approach, together with the Miner damage accumulation principle.
- The FDRS is then a plot of fatigue damage as a function of natural frequency (at various damping factors).

Assuming that stress levels ( $\Delta\sigma$ ) will be proportional to the response acceleration ( $a$ ) of the fundamental mass ( $m$ ) ( $\Delta\sigma = m \times a$ ) and combining this with the stress-life equation (Eq. 3-14) and the Miner equation (Eq. 3-22) yields the following expression for damage:

$$D = \left( \frac{m}{S_f} \right)^{-1/b} \sum n_i a_i^{-1/b} \quad \text{Eq. 3-25}$$

The constants before the summation will cancel in a relative damage calculation and therefore again only the fatigue exponent ( $b$ ) is unknown. As discussed in paragraph 3.4.2.4.3, a reasonable estimate can be made.

Olofsson describes an alternative cycle counting method to the rainflow method, called the HdM model, claimed to provide better results when stress histories are irregular and is easier to use. Counting of up crossings at levels of  $a$  ( $n_+(a)$ ) is performed. The summation is then changed to an integral:

$$D = \int_{a_{\min}}^{a_{\max}} n_+(a) a^{-1/b} da \quad \text{Eq. 3-26}$$

It is proposed that this formulation be used in design codes to specify fatigue loading. Enveloped curves, based on extensive measurements, will have to be used. Accelerations would typically be measured on bogeys and kingpins (rigid areas) and would thus be somewhat vehicle dependent. The curves would be normalised to exclude the  $S_f$  and  $b$  constants required to determine absolute fatigue damage. The practical use of such curves would therefore require the calculation of the first natural frequency of the tank structure under consideration, an estimation of the damping factor, as well as the determination of  $S_f$  and  $b$  for all critical points on the structure. Fatigue damage estimates, taking into account the simplified dynamic response of the structure, would then result. The method is depicted on the summary framework in Figure 3-17.

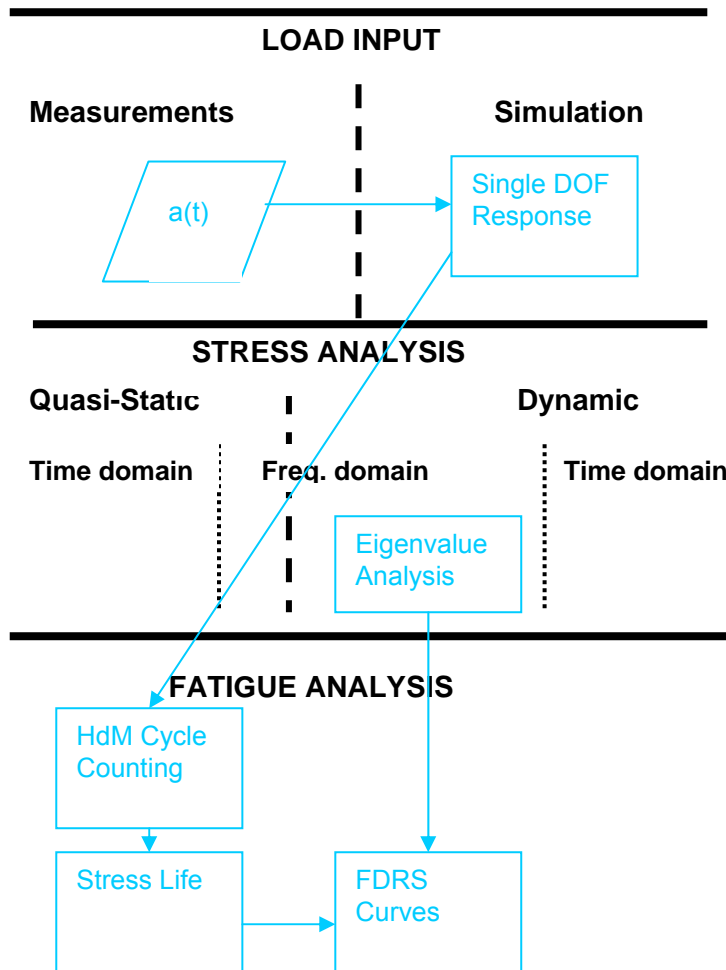


**Figure 3-17: Fatigue Damage Response Spectrum (FDRS) Method**

The methodology was not implemented as presented above by the present author for any of the case studies. For the light commercial vehicles, the dynamic response of the vehicles was inherently taken into account due to the fact that dynamic testing was performed. For the road tankers and the LHDs, it was demonstrated that the first natural frequency response would cause stress patterns proportional to those caused by static vertical inertial loading and that no other modes significantly contributed.

For the LTV industrial vehicle, higher order mode shapes were taken into account using the modal superposition method. In the latter case, there was no need to establish generic design criteria, which meant that the higher order mode excitation could be taken into account directly. In the case of the tank container, generic design criteria (valid for other designs), were required, a quasi-static methodology was followed, resulting in fatigue equivalent static g-loads. The above technique, however, may suitably address higher order dynamics in a way that would be generic for all designs and was therefore included into the generalised methodology formalised during this study.

### 3.6 CLOSURE

In this chapter, the fundamental theory underpinning the techniques applied for the case studies presented in the following chapters, was presented. Also dealt with were current practices with regard to the determination of input loading for vehicular structures.

Figure 3-18 depicts the summary framework, populated with all the durability analysis (as opposed to testing) methods described in this chapter. The diagram offers an holistic view of the different choices of methods and their relationships with each other. The advantages and disadvantages of the various methods are listed in Table 3-4. The colours used for each method in the diagram are listed in the legend column of the table. Black is used in the diagram for objects that are part of more than one method. The diagram and table are later employed to compare the newly developed methods employed during the present study, with the existing methods.

**Table 3-4: Comparison of Durability Analysis Methods**

	Type	Load Input	Stress Analysis	Fatigue Analysis	Legend	Advantages	Disadvantages
<b>Multi-body Dynamic Simulation</b>	Time domain	Road profile or measured accelerations	NA	NA	Dark green	May be used to obtain force inputs for FEA from measured accelerations or road profiles	Complex tyre models
<b>Remote Parameter Analysis</b>	Quasi-static, time domain	Straingauge measurements	Static FEA	Rainflow counting + various fatigue life analysis methods	Brown	Can use remote measured straingauge data, economic FEA	Not suitable for complex dynamic response, rainflow on each stress point, loading results not suitable for code = not design independent
<b>Co-variance method</b>	Quasi-static, frequency domain	Measured /simulated input forces	Static FEA	Dirlik formula + various fatigue life analysis methods	Light green	Takes account of complex dynamic response, economic FEA	Requires stationary random input data, Dirlik formula approximations, loading not design independent
<b>Random Vibration</b>	Dynamic, frequency domain	Measured /simulated input forces	Eigen value FEA	Dirlik formula + various fatigue life analysis methods	Pink	Takes account of complex dynamic response, economic FEA	Requires stationary random input data, forces must be measured, Dirlik formula approximations, loading not design independent
<b>Fatigue Domain Reponse Spectrum</b>	Dynamic, fatigue/frequency domain	Measured accelerations	Eigen value FEA	HdM cycle counting + Stress Life	Light blue	Takes account of complex dynamic response, economic FEA, loading is design independent	Requires stationary random input data
<b>Modal Superpositon</b>	Dynamic, time or frequency domain	Measured /simulated input forces	Eigen value FEA	Dirlik formula + various fatigue life analysis methods	Violet	Takes account of complex dynamic response, economic FEA	Forces must be measured, Dirlik formula approximations, loading not design independent
<b>Direct Integration with Large Mass, Relative Inertial, La Grange Multiplier</b>	Dynamic, time domain	Measured accelerations	Dynamic FEA	Rainflow counting + various fatigue life analysis methods	Orange and Red	Takes account of complex and transient dynamic response, accelerations may be measured, can be design independent	Expensive FEA

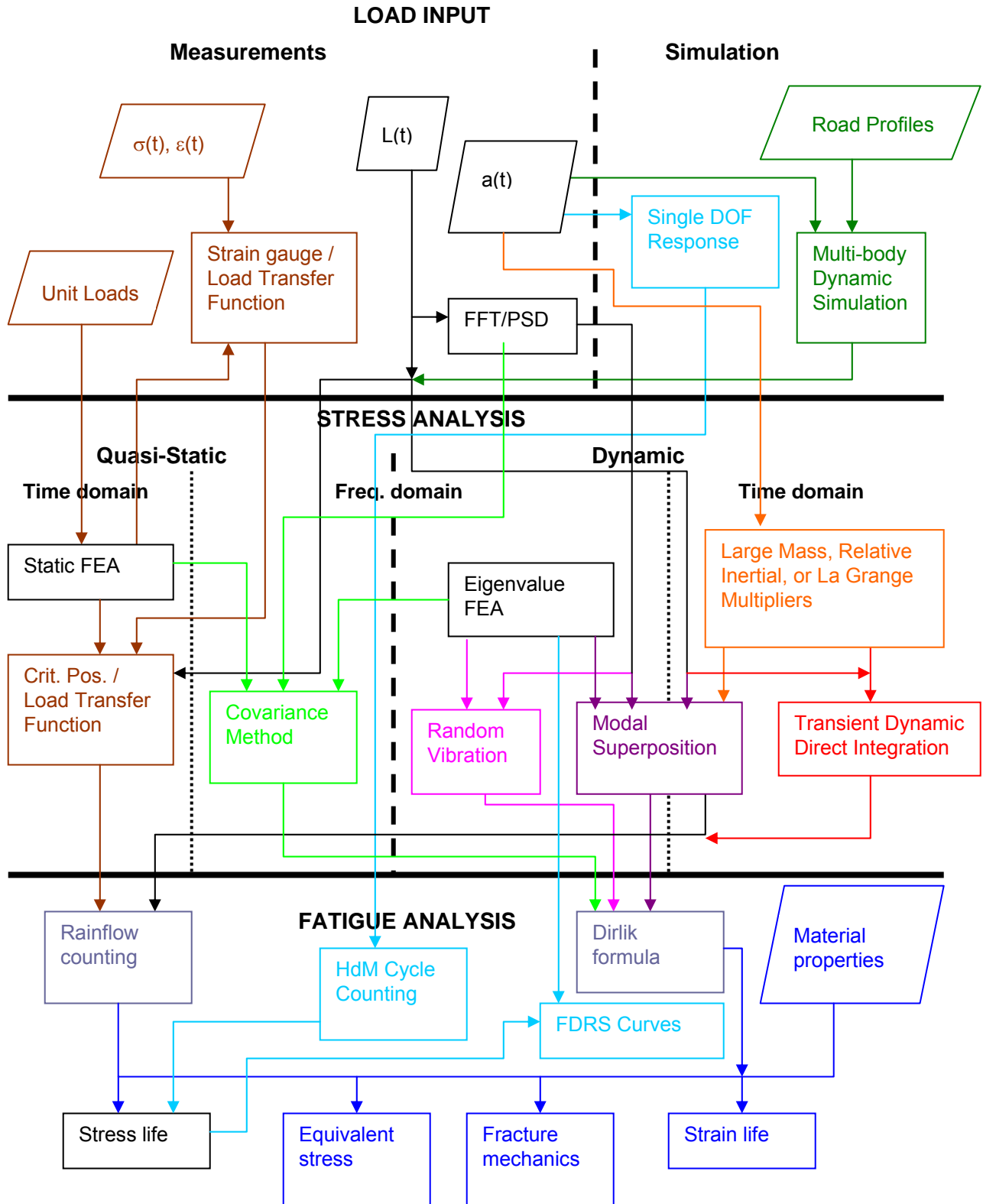


Figure 3-18: Summary diagram